NM WRRI Student Water Research Grant Final Report

1. Student Researcher: Edirisooriya, E.M.N.T. (New Mexico State University)
   Faculty Advisor: Dr. Huiyao Wang (Department of Civil Engineering, NMSU)
   Dr. Pei Xu (Department of Civil Engineering, NMSU)

2. Project title: Solar reforming of microplastics in water for H_2 production and degradation using nanocomposite photocatalysts

3. Description of research problem and research objectives.

Plastic pollution is a world problem for long time. The term "microplastics" refers to any fragmented plastic material with sizes less than 5 mm. They can be broadly categorized into primary and secondary microplastics that are mostly used in personal care products, cosmetics, medicines, textiles or disintegrate from larger plastic products. Microplastics can be found in ocean, lakes, industrial wastewaters, and effluents of water treatment plants. Microplastics have also been found extensively in drinking water sources. More than 80% of tap water samples collected worldwide tested positive for microplastics [1]. A recent report in Science indicates that approximately 0.48–1.27 million tons of plastic debris enters ocean annually [2]. Microplastics have significant effect on human and ecology. Microplastics tend to absorb toxic chemicals and make chronic diseases such as cancer and consumed by fish and mammals. Endocrine-disrupting plasticizers like bisphenol A or phthalates, flame retardants, can be absorbed into our diets and bodies.

Removal of microplastics from water or wastewater is difficult, due to the intrinsic physical and chemical characteristics. Few studies suggest treatment technologies such as membrane bioreactor, activated sludge, hydro cyclone, coagulation, filtration are effective to remove microplastics with sizes >1 mm from aqueous solution. Large amounts of smaller microplastics still pass through the existing water and wastewater treatment processes. The microplastics in lower μm and nm ranges are of special concern because their bioaccumulation potential increases with decreasing size. Other physical, mechanical, or chemical processes can be used to remove or degrade microplastics such as membrane filtration, thermal, chemical or catalytic oxidation, but these technologies are expensive and often have high energy requirements. Therefore, the objective of this research is to develop efficient and sustainable method to degrade micro- and nano-plastics from water using photocatalysis while producing hydrogen (H_2) under solar reforming.

4. Description of methodology employed.

Photo-mediated catalytic degradation is an energy-efficient technique that uses sunlight to degrade microplastics in water. During photocatalysis, electrons are excited to the conduction band of the

photocatalyst by sunlight and reduce microplastics to H_2. The resulting holes in the valence band of the photocatalyst initiate the degradation process, which leads to polymeric chain breaking, branching, crosslinking, and complete mineralization. The key component of the photocatalytic system is the highly functional nanocomposite photocatalysts that can utilize the full spectrum of solar energy with high photocatalytic oxidation capacity. The first step of the project will focus on developing suitable and environmentally friendly photocatalysts. Previous studies have demonstrated fragmented microplastics in water have been degraded through visible light-induced plasmonic photocatalysts comprising of platinum nanoparticles deposited on zinc oxide (ZnO) nanorods (ZnO-Pt) [3]. UV-absorbing TiO_2-Pt photocatalyst, and the toxic CdS/CdOx quantum dots have been used in photo reforming microplastics [4]. In this study we will synthesize highly functional photocatalysts such as ZnO-Pt, TiO_2-Au, TiO_2-Pt, and graphene oxide/TiO_2/Au ternary nanocomposites using atomic layer deposition and hydrothermal deposition methods. The prepared photocatalysts will be characterized using scanning electron microscopy (SEM), transmission electron microscopy (TEM), X-ray diffraction (XRD), and energy dispersive X-ray spectroscopy (EDS). Based on material characterization we will extract the chemical composition and structural configuration to optimize each fabrication step.

Then the optimized catalyst will be used for photo reforming and degradation of microplastics in water. Fourier transformation infra-red (FTIR) spectroscopy will be used to analyze chemical structure of microplastics, before and after solar photocatalysis. Carbonyl index (CI) and vinyl index (VI) of photocatalyzed microplastics can be calculated to compare the performance of photocatalysts as an indirect quantification of the degree of degradation. The operating conditions for H_2 production will be optimized in terms of microplastics loading rate, dosage of photocatalyst, pH, and pre-treatment of microplastics.

5. Description of results; include findings, conclusions, and recommendations for further research.

Literature Review Report

Introduction

The objectives of water and wastewater treatment and design specifications are primarily based on nonspecific parameters such as suspended solids (SS), turbidity, total dissolved solids, organic contaminants (e.g., biochemical oxygen demand (BOD)), and metals. The contaminants that must be removed from the water are complex mixture of particulate and soluble constituents. Size distribution of the contaminants strongly affect the treatability of water [5]. Particles in waters have conveniently been grouped into operational size categories such as soluble (<0.001 μm), colloidal (0.001–1 μm), supra colloidal (1–100 μm) and settleable fractions (>100 μm) [6].

Anthropogenic particles are major classification of particles produced as a result of direct and indirect human activities [7]. Microplastics (MPs) considered to be the most substantial category of anthropogenic particles. Due to the accumulation of plastic debris released into the ocean (8 million tons of plastic entering ocean every year forming millions of micro plastics [8]) and after photodegradation, embrittlement and fragmentation due to wave action millions of micro and nano sized plastic particles are formed. These plastic particles considered to be highly stable and durable in the waters [9].

According to Google Scholar, studies on microplastic and nano plastics have rapidly increasing, showing a broad research interest (Figure 1).

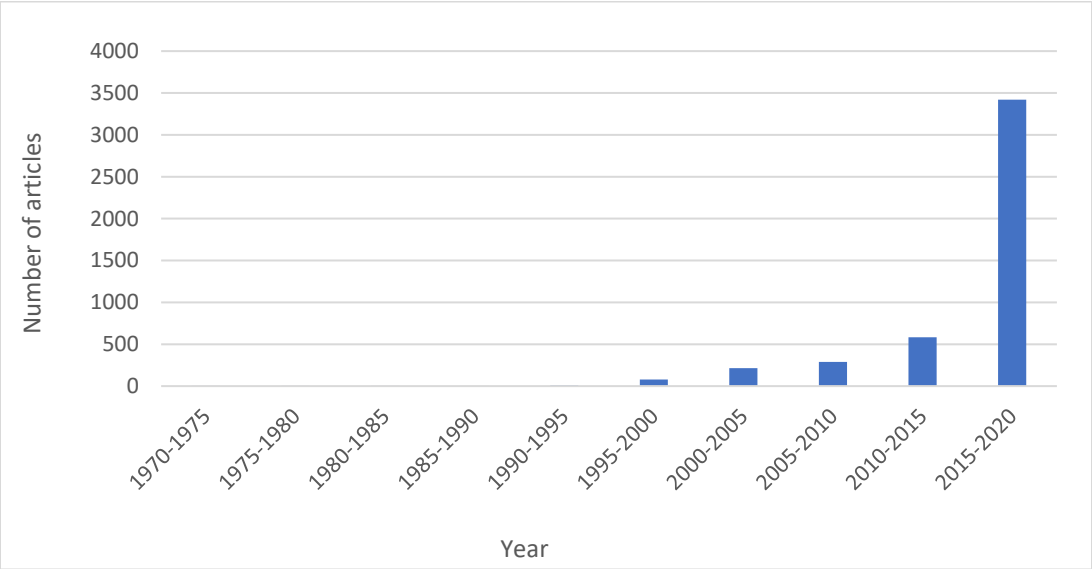

Figure 1: Variation of number of published articles with time (Source: Google Scholar)

Microplastics (MPs) refer to tiny plastic pieces, typically less than 5 mm in every dimension [10]. Microplastics can also be categorized according to its origin. Primary microplastics are raw materials for plastic products, for instance as resin pellets or as additives for personal care products such as shower gels and peelings. Secondary microplastics are degradation products broken down from larger plastic items, which are formed by UV radiation and physical abrasion to smaller fragments. Various compositions such as acrylic polyamide, polyester, high- and low-density polyethylene (HD/LD-PE), polyethylene terephthalate (PET), polypropylene (PP), polystyrene (PS), and polyvinyl chloride (PVC) are found in the aquatic environment. In addition, polyamide fibres (nylon) from fishing gears are frequent [11][12]. MPs consist of different shapes such as fibres, films, foams, foils, fragments, pellets and spheres. Different shape fractions of microplastics in wastewater have been studied [13]. Further, additives may be added to plastics to improve their characteristics such as strength, coloration or flame-retardant properties (e.g., Bisphenol A, phthalates, polybrominated diphenyl ethers, and metals or metalloids). Some of these additives have

been found to be carcinogenic or endocrine disrupting [14]. Figures 2 and 3 summarize the categories of microplastics and sources of MPs.

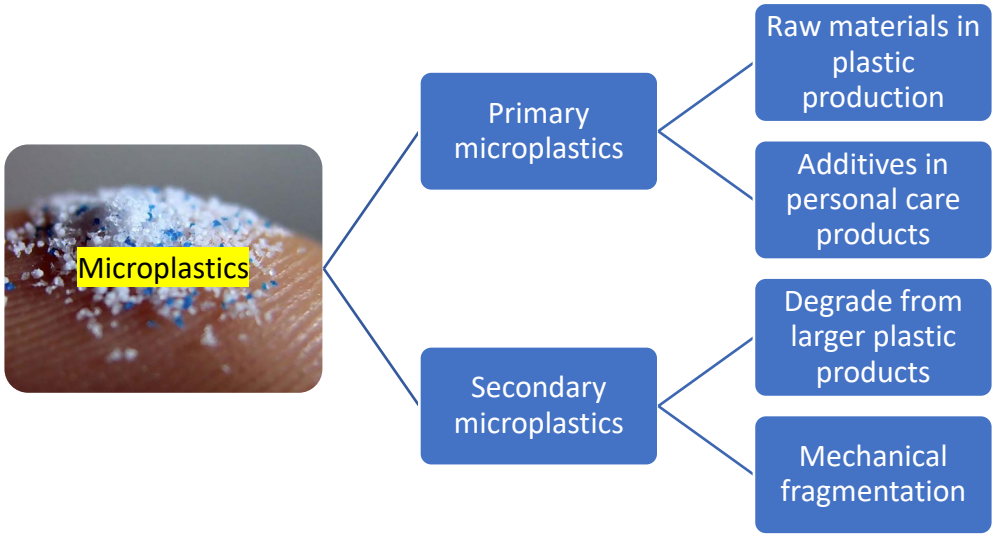

Figure 2: Categorization of microplastics

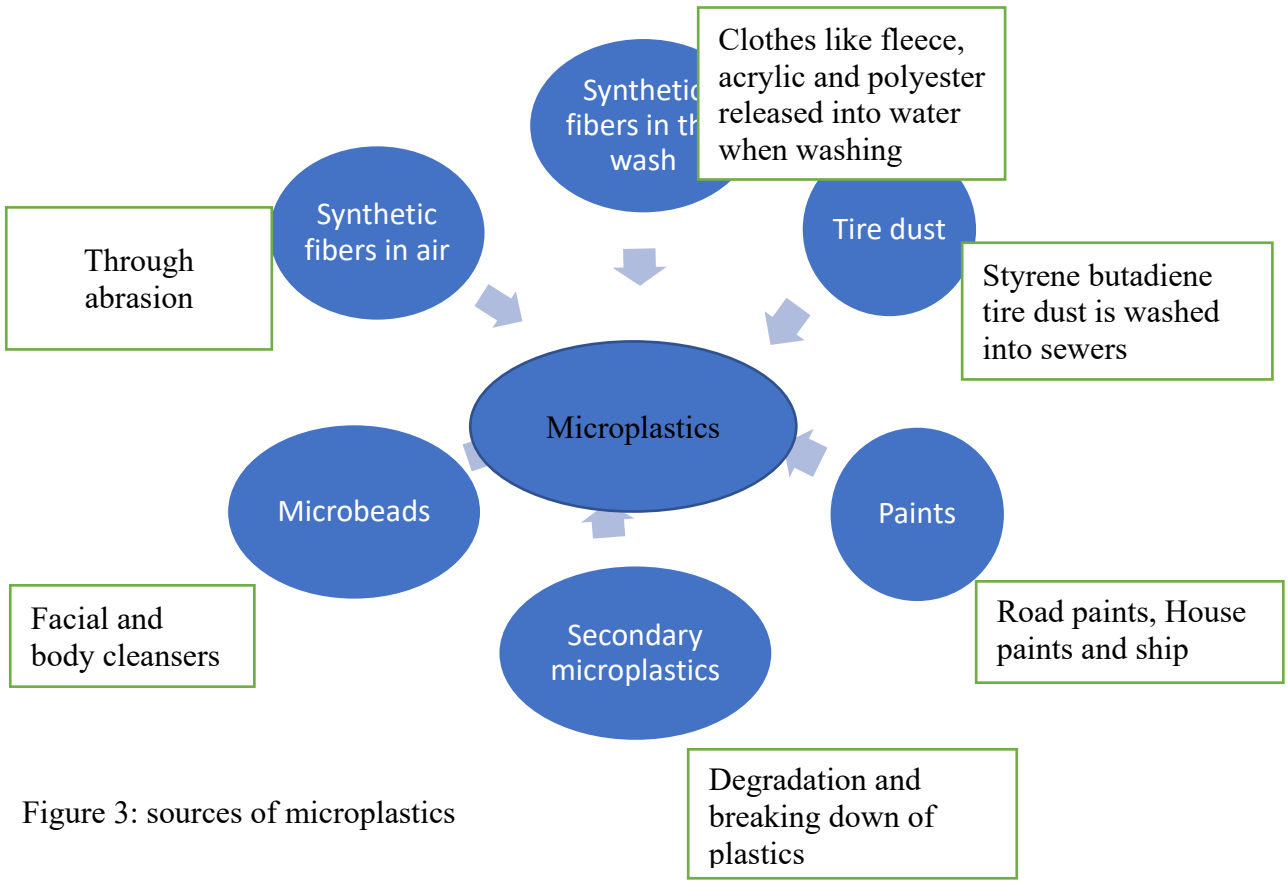

Figure 3: sources of microplastics

Smaller the particle size easier to be ingested by variety of organisms from small fish to large mammals. Microplastics are taken up by cells of blue mussel Mytilus edulis causing adverse effects on the tissues of the mussels. Further, MPs are ingested by zooplankton gather in salt and fresh water. These MPs tend to absorb toxic chemicals and lead to chronic deceases such as cancers [14], [15]. MPs can pass through the wastewater treatment plants and can present in soil and freshwater ecosystems [14]. MP can act as a vector for waterborne (human) pathogens influencing the hygienic water quality [11].

Nano plastics are defined as particles within a size ranging from 1 to 1000 nm resulting from the degradation of industrial plastic objects and can exhibit a colloidal behaviour. Nano plastics are highly polydisperse in physical properties and heterogeneous in composition. Nano plastics are formed when microplastics breakdown on their way to aquatic sources [16]. Dispersion and aggregation of nano plastics are influenced by the solution chemistry parameters such as pH, divalent cations and natural organic matter in fresh water [17]. Main properties that define nano plastics are listed in Table 1.

Table 1: Properties of Nano plastics [18]

Property	Description
Composition	Mixture of polymers, highly weathered
Size	1nm-1μm
Size distribution	Polydisperse (continuum of size)
Shape	Asymmetrical
Surface charge	Uncontrolled with the presence of different species
Stability	Hetero aggregation with other natural and/or anthropogenic colloids during the formation process; Depending of both nano plastics and its surrounding media physical and chemical properties
Porosity	Open structure

Toxicity of the micro and nano plastics

Toxicity studies are divided into two parts as acute toxicity and chronic toxicity. Further in vitro and in vivo studies are carried out to evaluate toxicity [19]. Brief introduction about acute and chronic toxicity studies is given in Table 2. Micro and nano plastics in water can cause both acute and chronic toxicity.

Table 2: Introduction on acute and chronic toxicity [20]

	Acute toxicity	Chronic toxicity

Definition	Single exposure or multiple exposures within short period of time	Development of adverse effects due to long term exposure
Test methods	Acute lethality test	Full life cycle tests: evaluate the effects of series of chemical concentration on reproduction, growth and survival of one or more generation of a test organism Partial life cycle/sensitive life stage tests Functional tests
Parameters	Median lethal concentration : concentration of chemical which kills the 50% of test organisms during the predetermined time Median effect concentration	No observed effect concentration (NOEC) Lowest observed effect concentration (LOEC)
Evaluation parameters	Mortality	End points (individual growth rate, abnormal development, hatching time and success, reproduction) Vitality of offspring Behaviour of individual and physiological parameters

The following factors should be considered when selecting test species for toxicity tests:

- Should be easy keep under laboratory conditions
- Easy to feed and breed
- Must have a large reference database

When considering the effect of microplastics, translocation of MPs across the gastrointestinal tract was reported. Translocation across the mammalian gut into the lymphatic system of various types and sizes of microparticles (between 0.1 and 150 mm) has been demonstrated in studies involving humans (0.2 and 150 mm). In dogs, PVC appeared in the portal vein, which will then reach the liver. Small intestinal uptake in rodents was shown after using 2 mm latex particles (0.3%). In a study conducted in vitro, limited absorption (0.2%) of polylactide-co-glycolide microparticles (3 mm) was measured in human mucosal colon tissue. The mucosal colon tissue of patients with inflammatory bowel disease, showed increased transport (0.45% as compared to 0.2% in healthy controls) in relation to greater gut permeability.

The physical presence of MPs may be toxic due to their inherent ability to induce intestinal blockage or tissue abrasion. In earthworms (*Eisenia andrei*), fibrosis, congestion and inflammatory infiltrates were observed after exposure to MPs (from 62 to 1000 mg/kg of PE). In sea bass (*Dicentrarchus labrax*), moderate to severe histopathological alterations of the intestine were measured, after 30-90 days of exposure to PVC MP through ingestion. According to the authors, damages recorded after 90 days of exposure could be responsible for totally compromising intestinal functions [14]. Table 3 shows the potential health impacts from different types of plastics.

Table 3: Potential health impacts from different microplastic types

Type of plastic	Description	Potential health impact
Polyethylene Terephthalate (PET)	Ubiquitous, durable plastic used to bottle water, juice and soda Safest plastic for food storage and easily recycled	Can leach antimony in amounts exceed U.S. safety guidelines when exposed to high temperature
High density polyethylene (HDPE)	Use to package (Milk, juice, water, cleaning supplies and shampoos)	Leach estrogenic chemicals when exposed to heat, boiling water and sunlight which cause breast cancer, endometriosis, altered sex ratios, testicular cancer, poor semen quality, early puberty and malformations of the reproductive tract.
Polyvinyl Chloride (PVC)	Wraps meat and sandwiches, floats in the tub in the form of bath toys, makes for stylish jackers and household plumbing	Leaches toxic chemicals when in contact with water. Four chemical softeners used with PVC. These chemicals interfere with the body's production of hormones
Low density polyethylene (LDPE)	Used in shrink wrap, milk cartons, take out coffee cups and to package sliced bread, newspapers and dry cleaning	LDPE is considered a low hazard plastic
Polypropylene (PP)	Make containers for yogurt, takeout lunches, medicine and syrups.	Fairly safe plastic
Polystyrene	Expanded polystyrene foam is widely used for takeout food and in the fishing industry	Human carcinogen can leach from polystyrene in contact with hot beverages

Toxicity studies of nano plastics was conducted using Cladocera species (*Daphnia magna*) as aquatic model organism. The study suggests that acute toxicity and physical damage to Daphnia magna is associated with the solution chemistry parameters and the particle surface modification. Further, more complex the solution conditions, more toxic the plastic nano particle (Zhang et al., 2019).

Methods of characterization of the plastic particles

Physical characterization methods

Physical properties of particles can be characterized as particle size, shape, density and viscosity. Steric field flow fractionation (FFF) is one technique of identifying these properties in 1-100 μm range of particles. The theory of steric FFF is based on different elution mechanisms of organic matter in terms of sizes. The procedure uses the laminar flow exists in measuring channel and particulate organic matter is separated by size in the flow streamlines [21].

Dissolved organic carbon (DOC) less than 0.45 μm can be separated by dialysis, laser desorption Fourier transform mass spectrometry, vapour pressure osmometry, ultracentrifugation, X ray scattering, ultrafiltration technique and gel permeation chromatography [22], [23]. Separation of DOC by dialysis is simple and the main process applied is diffusion. However, it is a time-consuming process which requires large sample volumes.

The granulometry technique was also used to measure the distribution of the particle size. This technique was carried out using a Malvern Mastersizer 2000LF laser with a Malvern HYDRO 2000Up minimum volume liquid sample dispersion unit, which measures the size distribution in a range of 0.02–2000 μm [24].

Chemical characterization methods

Chemical identification of particles (microplastics) is commonly done using Fourier transform infrared (FTIR) and Raman spectroscopy. By vibrational spectroscopy, molecule vibrations of a sample are excited and detected, which leads to characteristic spectral fingerprints in the FTIR or Raman spectra. Thus, a characterisation based on the polymeric chemical structure and identification by comparison with known reference spectra becomes possible. Using FTIR spectroscopy the sample is irradiated with IR light (wavenumber range 400–4000 cm^{-1} for Mid-IR). A part of the IR radiation is absorbed depending on the molecular structure of the sample and finally measured in transmission or reflection mode [25].

Raman spectroscopy is a scattering method in which monochromatic light (laser) as source is used. The radiation interacts with the sample. A small part of the scattered photons has an energy shift and gives information about molecule vibrations in the sample. The resulting Raman spectrum provides similar information as an IR spectrum. There is, however, a fundamental physical difference between FTIR and Raman spectroscopy. Briefly, IR absorption depends on the change of the permanent dipole moment of a chemical bond leading to the fact that polar functional groups (e.g. carbonyl groups) are very well detectable. On the other hand, Raman spectroscopy depends on a change in the polarizability of a chemical bond, whereby e.g. aromatic bonds, C–H and C=C double bonds can easily be excited. Hence, FTIR and Raman spectroscopy are complementary

vibrational techniques, meaning that bands which have strong Raman intensities in many cases have weak IR intensities and vice versa. These physical fundamentals should be considered when FTIR and Raman spectroscopy are applied for the microplastics topic [25]. Table 4 indicates a comparison between FTIR and Raman spectroscopy.

Table 4: Comparison of FTIR and Raman spectroscopy

FTIR	Raman spectroscopy
Measures absorption of radiation	Monochromatic laser layer impinges onto a sample
Spectrum is produced: spectrum indicates the energy of radiation absorbed by the molecule	Scattered photons are created
Lower spatial resolution	Higher spatial resolution
Good performance in smaller particle Identification	Better performance when identifying particles down to 1 μm
Used in 28% of MP identification studies	Used in 14% of MP identification studies
	Subject to fluorescence or sample degradation by photodecomposition or heating and allows different frequencies of lasers
Spectral libraries are used to match the spectra from unknown material	Spectral libraries are used

Spectral Library of Plastic Particle (SLoPP) and Spectral Library of Plastic Particles aged in the Environment (SLoPP-E) are created including databases of suggested analytical parameters in order to gather enough details to identify particles using Raman spectroscopy [26].

Nile Red staining with UV microscopy (for sizes between 6.5 and 100 μm) was performed to identify the particles and the results were corrected for background laboratory contamination levels using a series of blanks. Chemical composition of materials also can be characterized using micro x-ray fluorescence analysis (XRF spectroscopy). It is a non-destructive analytical method [27].

Morphological characterization methods

Particle morphology can be easily investigated by the electron microscopy, atomic force microscopy (AFM), and optical techniques. Scanning transmission X-ray microscopy (STXM) was used to identify the morphology of particles in pH changing aqueous solution [28]. Microscopic methods can be used to investigate particles in the size range of 0.001—200 μm. There are two methods in electron microscopy namely scanning electron microscopy (SEM) and Transmission electron microscopy (TEM) based on the energy of involved electrons and the way of electron collection. TEM can be used to analyze particles ranging from 0.001-5 μm and SEM can analyze particles with size range of 0.02- 200 μm. TEM can show the internal structure of particles, hence

provide more detailed characterization. SEM probes the surface of particles which are first covered with a very thin layer of gold and then bombarded by electrons. These methods considered to be costly and time consuming [5]. Further, scanning electron microscopy-energy dispersive X-ray spectroscopy (SEMEDS) and environmental scanning microscopy-energy dispersive X-ray spectroscopy (ESEM-EDS) can also be used for characterizing surface morphology [29]. Further, SigmaScan 5 software (Systat Software, Inc., USA) was used to determine morphology of microplastics in water.

Structural characterization methods

Light scattering is one of the most common technique used in particle characterization. Both dynamic light scattering (DLS) and static light scattering (SLS) have been applied for characterization. Temperature sensitivity and structure of particle are studied using DLS. Further, NMR or pulsed gradient spin echo (PGSE) NMR spectroscopy was recently used to study the heterogenous structure inside the particles [28]. High-pressure size exclusion chromatography (HPSEC) is a powerful technique for determining molecular weight (MW) distributions of aquatic humic substances. HPSEC is non-destructive, relatively fast and does not require to pre-treat the samples [30].

Specific UV absorbance at wavelength of 254 nm ($SUVA_{254}$) is an indicator of the hydrophobic organic acid fraction of dissolved oxygen matter [31]. High SUVA value indicates that the organic matter is largely composed of hydrophobic and high molecular mass (MM) organic material. Low SUVA value indicates that water contains mainly organic compounds which are hydrophilic, of low MM and have low charge density.

Comparison of different characterizing methods with their advantages and disadvantages is summarized in Table 5.

Table 5: Comparison of different characterizing methods

Technical method	Advantage	Disadvantage
Dialysis	- Simple application - Natural force (diffusion)	- Time consuming - Large sample volume required - Limited range of size distribution (2 – 5 nm) - Careful handling of membrane
LDFTMS	- Independent on the material being characterized - Relatively accurate size	- High power required - Concentrated samples required - Small MW measured

VPO	- Limited range of size distribution - Yield only a number-average MW - Corrections for ionizable compounds	
Ultracentrifugation	- Various molar mass (Mw, Mn, and Mz)	- Diffusion coefficient required - Swamping of charge effects; absorptivity varies with MW
UF	- Relatively inexpensive - nondestructive and regent-free - Simple application - High reliability	- Effect of self rejection - Broad range of size distribution - Large sample volume required - Influence of ionic strength, pH and concentration polarization - Difficult separation with high concentration
Flow FFF	- Identification of interaction between membrane and OM	- Sorption on the membrane
HPSEC	- Small sample volume required - Specific range of size distribution - Automatic analysis - A number of compatibilities - Relatively inexpensive	- Errors due to chemical interactions among OM, column packing and eluent - Electrostatic interaction - Sorption - Calibration required - Specific analysis depending on detectors used - Effect of pH

Microplastic removal

Microplastic removal from aqueous media has been studied using different technologies such as membrane bioreactors, retrofiltration and bacterial oxidation [3]. Final stage wastewater treatment techniques such as membrane bioreactor, rapid sand filter and discfilter were studied to identify their suitability to remove microplastics and treatment efficiencies were reported as 99.9%, 97% and 95% for membrane bioreactor, rapid sand filter and discfilter respectively. Filtration was found to be unsuccessful due to clogging and isolation of particles using acidic digestion also failed due to excessive solid loads [32]. Analysis of samples taken from multiple locations within treatment plants showed that most of these contaminants were removed at the primary treatment stages via skimming and settling processes. Tertiary WRP processes appear to be effective at removing microplastic contaminants in their influents, even the secondary downstream wastewater/solids handling facility showed removal efficiency above 99.9%. Our findings also reveal that some consumer products may be contributing disproportionately more than others to WWTP microplastic loads [32].

Coagulation process was applied to remove microplastics from water and effect of different pH conditions and different coagulants have been studied. Al-based coagulants found to be most effective in removing microplastics than Fe-based coagulants. With conventional dosages low removal efficiencies have been shown. Ionic strength, concentration of natural organic matter and turbidity level showed a lower influence on removal efficiency. In the ultrafiltration process studied in the same study high removal efficiency was observed. However, membrane fouling induced after coagulation with Al-based salts at a conventional dosage, especially for the large PE particle size. The removal behaviours of microplastics exhibited during coagulation and ultrafiltration processes have application potential for drinking water treatment [33].

Microplastics are transported to the surface of the flocs due to their buoyancy and floating matter is then removed by skimming device in wastewater and water treatment plants. Further, conventional wastewater treatment plants (WWTPs) have shown an ability to remove a portion of the plastic MPs, however, large amounts still pass through the process, accounting for up to hundreds to thousands of particles per m^3 effluent [12], [34].

To estimate the number of MPPs in raw influent, assembled sieve cascade (mesh size: 9.5 mm-180 mm) was used to sieve the influent flows. Unfortunately, these filtration attempts failed because the sieves were rapidly clogged by paper and other solid residues in the raw influent. Attempts to isolate particles by utilizing acidic digestion also failed because of excessive solid loads. We then tried to isolate any MPPs by exploiting their inherent buoyancies. This was performed by sparging 5 L of influent for 4 h in a large beaker [35]. Further, bio-coatings may act as wetting agents and may modify the surface properties of hydrophobic polyethylene fragments, or the biofilm could alter the particles' relative densities compared to that of “clean” or uncoated plastics. Any such changes could measurably impact removal efficiencies of MPPs at municipal treatment plants.

Grbic et al used a magnetically extraction method to remove microplastics from different water samples. Hydrophobic Fe nanoparticles were used to magnetize microplastics. 92% of 10- 20 μm sized polyethylene and polystyrene beads and 93% of >1 mm MPs (polyethylene, polyethylene terephthalate, polystyrene, polyurethane, polyvinyl chloride, and polypropylene) were removed from seawater. 84% and 78% of MPs from freshwater and sediments respectively was also removed in the size category of 200 μm and 1 mm [36]. While technologies exist to filter microplastics, they can often be expensive and difficult to install into wastewater treatment plants and often go unimplemented unless effluent quality standards are high. It was determined that two main factors influenced the effectiveness of filtration of microplastics: filter material and pressure [15]. Researchers found that centrifugation may lead to compacting, deforming and breaking down of microplastic particles and microwave digestion is likely to lead to decomposition of microplastics, and the effects of enzymatic digestion on infrared spectra have not been fully studied. PS bead removal efficiencies of water using magnetic Polyoxometalate-Supported Ionic Liquid Phases

(magPOM-SILPs) is over 90% based on DLS analyses. This emphasizes that the magPOM-SILPs are capable of removing microplastic model compounds from large volumes of water [37]

Liu et al. used a pilot scale biofiltration technique to remove MPs from treated wastewater and 79% of overall removal efficiency was achieved. Results of the study suggest that microplastics larger than 100 µm tend to remove and smaller particles are released into the environment [38]. Data from over 70WWTPs has shown that although the inclusion of tertiary treatment processes (TTPs) highly reduces the average amount of microplastics in the effluents, this can still be as high as 51 particles L^{-1}, and only approximately 24% of WWTPs incorporate TTPs [39]. Granular activated carbon filtration performed well in microplastic removal with efficiency of 56.8% to 60.9% [40].

Extracellular polymeric substances (EPS) production by bio algae, *Cyanothece sp.* with exposed to micro and nano plastic mixed environment was studied. The results showed that polystyrene nano- and microplastics (at 1 and 10 mg L^{-1}) had a significant negative impact on the growth of this freshwater microalga. The production of extracellular carbohydrates was shown to be largely enhanced in the presence of nano- and microplastics. Also, EPS production was significantly higher when exposed to 10 mg L^{-1} of PS nano-plastics. *Cyanothece sp.* produces EPS with high bio flocculant activity in relation to the low concentration tested, which is suitable for nano- and microplastics aggregation, displaying hetero-aggregation potential at 1 and 10 mgL^{-1} of both nano- and microplastics. The results of this investigation highlight the promising potential for microalgal-based biopolymers to replace the hazardous bio flocculants used in wastewater treatment, in addition to the ability to aggregate the <300 mm microplastics fraction that conventional removal methods in wastewater treatment are unable to remove [39].

Advanced oxidation mechanisms can be classified as homogeneous or heterogeneous photocatalysis. Homogeneous photocatalysis employs Fenton's reagent, which is a mixture of hydrogen peroxide and an Fe^{2+} salt to produce hydroxyl radicals under UV irradiation at wavelengths above 300 nm. However, heterogeneous photocatalysis employs semiconductor oxides as a photocatalyst. Among semiconductors, titanium dioxide (TiO_2) has been the most studied compound in past decades. Owing to its low production cost and good chemical stability, it has been widely employed in photo-degradation of organic compounds, such as those with a high loading of nitrogen-containing organic compounds saturated hydrocarbons (alkanes), aromatic hydrocarbon, non-biodegradable azo dyes, volatile organic compounds and pesticides with a UV light source [41].

Heterogeneous photocatalysis has been applied in water treatment and air pollution control. In the process of photocatalysis many pollutants in the water are breakdown at the room temperature by oxidation. Either sunlight or artificial light is used as energy source.

Photocatalytic membrane reactors (PMR) are developed with advancing technology while coupling photocatalytic activity with nano or ultrafiltration technology. The advantages of PMR with a photocatalyst immobilized on a membrane substrate are;

- No extra photocatalyst recovery steps.
- Stable flux and low flux-decline rate.
- Contaminants could be decomposed, either in feed or in permeate
- Mitigation of membrane fouling due to the decomposition of organic contaminants and enhanced hydrophilicity of the modified membrane [41].

Photo-reforming of plastic waste has been identified as efficient method of recovering H_2. Photo-reforming requires four components such as photocatalyst, substrate, sunlight and water. Electrons are excited to the conduction band (CB) of the photocatalyst by sunlight and reduce water to H_2. The resulting holes in the valence band (VB) of the photocatalyst oxidise the substrate to smaller organic molecules that remain in solution.

It is required to provide additional step to recover catalyst from suspended photoreactive process. However, hybrid photocatalytic membrane process does not require a complicated recovery of photocatalysts after water treatment. This hybrid technology uses stationary nanostructured photocatalysts to enhance the absorption of photons and reactants so that the catalyst does not need to be suspended in solution [41].

Currently, the contribution of the WWTPs to the discharge of large amounts of microplastics into the environment is still a debate between the authors. Also, the lack of standardization on the methodology applied to collect and interpret data makes it more difficult to reach a common sense about the link between microplastic pollution in aquatic systems and the WWTPs.

Transport and fate in water and wastewater treatment facilities

During the flotation, microplastics are transported to the surface of the flocs due to their buoyancy. The floating matter is then removed by skimming device. As flotation is particularly designed to remove low-density particles, it can be expected to efficiently remove plastics, at least those that have lower density than water.

During the DF 10 μm sampling, the varying quality of the pilot influent led to excessive polymer additions, which in turn caused the volume differences between the replicates after the treatment, as sticky polymer flocs blocked the filters quickly. The excessive polymer addition also resulted in membrane fouling in the discfilter pilot, which led to accelerated backwash frequency. During the high-pressure backwash, part of the MPs probably passed the filter.

The high counts of microplastics discovered at the skimming troughs confirmed the presence of microplastics in the WRPs influent. Conventional wastewater treatment plants (WWTPs) have shown an ability to remove a portion of the plastic MPs, however, large amounts still pass through the process, accounting for up to hundreds to thousands of particles per m^3 effluent ([12]), while smaller particles are less likely to be retained by the treatment plants ([42].

Advanced oxidation processes

Advanced Oxidation Processes (AOPs) have been studied as alternative technologies for the treatment of contaminated water and wastewater. Most AOPs rely on the formation of hydroxyl radicals (HO), which are very reactive and non-selective oxidizing species capable of degrading an extensive variety of organic pollutants. One such AOP is the vacuum UV(VUV) process, which relies on the high energy photons generated by VUV lamps, emitting radiation at wavelengths lower than 200 nm. Ozone-producing low-pressure Hg lamps, which emit about 10% 185 nm radiation (VUV) and about 90% 254 nm radiation (UV), are one alternative for providing the necessary radiation. Excimer lamps, on the other hand, can emit quasi-mono- chromatic radiation at 126, 146, 172, 222, 282, or 308 nm, depending on the type of gas used in the lamp. Hg lamps have lower cost and provide similar electrical efficiencies compared to excimer lamps [43]. The VUV/UV process offers the advantage of no chemical or catalyst addition which in turn translates into simpler and more sustainable operation along with potentially lower operating cost. CFD model for simulating VUV/UV photoreactors was developed and evaluated against experimental data [44].Table 6 and 7 represent the advance oxidation process classification and different semiconductor materials as photocatalysts and their properties respectively.

Table 6: Advanced Oxidation Process

Homogeneous Photocatalysis	Heterogeneous Photocatalysis
Employs Fenton's reagents	Employs semiconductor oxides as photocatalysts

Table 7: Different semiconductor materials as photocatalysts and their properties

Semiconductor	Properties
TiO_2	Low production cost Good chemical stability Application of TiO_2 using solar energy is highly restricted by its large band gap (3.2 eV) and low quantum efficiency
ZnO	n- type semiconductor. Higher absorption efficiency across a large fraction of the solar spectrum when compared to TiO_2. Nonstoichiometric of ZnO rendering it a better photocatalyst compared to TiO_2 under solar irradiation.

	Large excitation binding energy (60 meV). Deep violet/borderline ultraviolet (UV) absorption at room temperature. Antifouling and antibacterial properties. The main drawback for ZnO semiconductors as photocatalysts is their low-charge separation efficiency.

Heterogeneous photocatalytic oxidation steps can be explained as,
1. Organic pollutants diffuse from the liquid phase to the surface of ZnO.
2. Adsorption of the organic pollutants on the surface of ZnO.
3. Oxidation and reduction reactions in the adsorbed phase.
4. Desorption of the products.
5. Removal of the products from the interface region.

Synthesis

Divided into solution-based and vapor phase approaches. Morphology of the nanostructures can be easily controlled by manipulating the experimental factors such as type of solvents, starting materials and reaction conditions. Solution-based approaches to synthesize ZnO nanostructures including hydrothermal, sol-gel, precipitation, microemulsion, solvothermal, electrochemical deposition process, microwave, polyol, wet chemical method, flux methods and electrospinning. Sol-gel technique is the most attractive method for ZnO nanostructure synthesis because of its low production cost, high reliability, good repeatability, simplicity of process, low process temperature, ease of control of physical characteristics and morphology of nanoparticles, good compositional homogeneity and optical properties.

Vapor phase approaches include thermal evaporation, pulsed laser deposition, physical vapor deposition, chemical vapor deposition, metal-organic chemical vapor deposition (MOCVD), plasma enhanced chemical vapor deposition (PECVD) and molecular beam epitaxy (MBE). Among them, some methods utilize metal catalysts to control the growth of nanostructures.

The synthesis of functional nanoparticles via one-step flame spray pyrolysis (FSP), especially those of catalytic nature, has attracted the interests of scientists and engineers, as well as industries. The rapid and high temperature continuous synthesis yields nanoparticles with intrinsic features of active catalysts, that is, high surface area and surface energetics. For these reasons, FSP finds applications in various thermally inducible catalytic reactions. However, the design and synthesis of photocatalysts by FSP requires a knowledge set which is different from that established for thermal catalysts. Unknown to many, this has resulted in frustrations to those entering the field unprepared, especially since FSP appears to be an elegant tool in synthesising oxide nanoparticles of any elemental construct.

Synthesizing methods for TiO_2 nanostructures,

1. Hydrothermal Method
2. Solvothermal Method
3. Sol-Gel Method
4. Direct Oxidation Method
5. Chemical Vapor Deposition
6. Electrodeposition
7. Sonochemical Method
8. Microwave Method

Table 8 shows the removed polymer and the catalyst used in several studies

Table 8: Summary of removed polymers and used catalyst in several studies

Study	Polymer type	Catalyst	Reference
Visible light photocatalytic degradation of microplastic residues with zinc oxide nanorods	low-density polyethylene (LDPE)	Zinc Oxide nanorods	[3]
Photo reforming of Nonrecyclable Plastic Waste over a Carbon Nitride/Nickel Phosphide Catalyst	PET and poly (lactic acid)	Carbon Nitride/Nickel Phosphide Catalyst	[4]
Plastic waste as a feedstock for solar driven H_2 generation	polylactic acid, polyethylene terephthalate (PET) and polyurethane	CdS/CdO_x quantum dots	[8]

Summary

Microplastics are defined differently by researchers and this lack of solid definition of what can be considered as microplastic makes it difficult to compare the results obtained in different investigations. Also, there are differences between the methodologies applied on the studies; hence, the results are not always comparable between themselves. When considering, results from examining tertiary treatment effluents suggest that, the low sample volumes together with low MP concentration and sensitivity to contamination leads easily to false estimation of MP concentrations in effluents. Recent studies emphasize the necessity of standardized and harmonized methods when evaluating the amount of MPs discharged from WWTPs. Membrane bioreactors are an example after primary and secondary treatment, using cross-flow filtration, diffusing only water and small particles. Another drawback of this technology is the high demand for energy and hence higher cost of operation. Additionally, only a small number of suspected microplastic particles have been spectroscopically confirmed due to the high cost of analysis as wastewater laboratories do not

normally possess FTIR or Raman spectrometers. Furthermore, microplastics have only been identified by using available, standard libraries. For a more accurate confirmation, obtaining spectra from reference microplastic standards may be necessary [10]. Most of the researches addressed to a specific type of microplastic or separately remove the specific type (PET, PP); but microplastic present in water is a mixture of many polymers. Then finding a photocatalytic with optimal removal efficiency for all the polymers will be required. Up to now, a series of detecting methods have been investigated for identifying microplastics. However, owing to the complexity of water conditions, no satisfactory method has been established. Earlier studies employed toxic, Cd-based quantum dots as the photocatalysts, and the plastics mixtures were converted into intractable organic both of which are undesirable. Moreover, they only achieved conversions of about 40% for specific plastics such as polyurethane and polyethylene terephthalate, and their process, required alkaline pre-treatment to partially hydrolyse the carbamate and ester link ages. Though Reisner and co-workers' most recent work on the photo reforming of plastics with CN_x/Ni_2P catalysts presents an innovative advance that overcame the toxicity of their original Cd-containing photocatalysts, their process still required alkaline pre-treatment, while conversions remained below 50% and multiple products with modest selectivity were observed [4].

Photocatalytic LDPE oxidation led to formation of low molecular weight compounds like hydroperoxides, peroxides, carbonyl and unsaturated groups, resulting in increased brittleness along with wrinkles, cracks and cavities on the LDPE surface" [3]. Hence study suggest finding less harmful by-products creating technologies. Further it is required to find suitable catalyst which create less harmful by-products. Or else by-products treatment methods should be identified and applied. Despite some advances, a clear path toward improvement in charge separation is still missing, resulting in quantum efficiencies that are still low, even in the best existing photocatalytic systems" [45]. Hence studies suggest improving the photocatalytic systems and find different structures, methods of improving and cocatalysts.

Additionally, photocatalyst itself is a harmful substance which is anthropogenic and should avoid the contamination. So that recovery processes should be applied while optimizing the efficiency. The development of selective oxidation cocatalysts remains a key challenge for polymer Photo-Reforming (PR). To enhance the real-world applicability of plastic PR, future work must focus on key bottlenecks including catalyst efficacy, conversion rates and selectivity, substrate solubilization, reduction or reuse of KOH, and reactor design [4]. Stability of the photocatalytic material also effect when industrially applying the process. Recovering the photocatalytic from the media is another drawback that need to be addressed. Catalyst immobilized in polymeric membrane have been proposed as potential solution to this matter.

Methodology

Schematic diagram of experimental plan

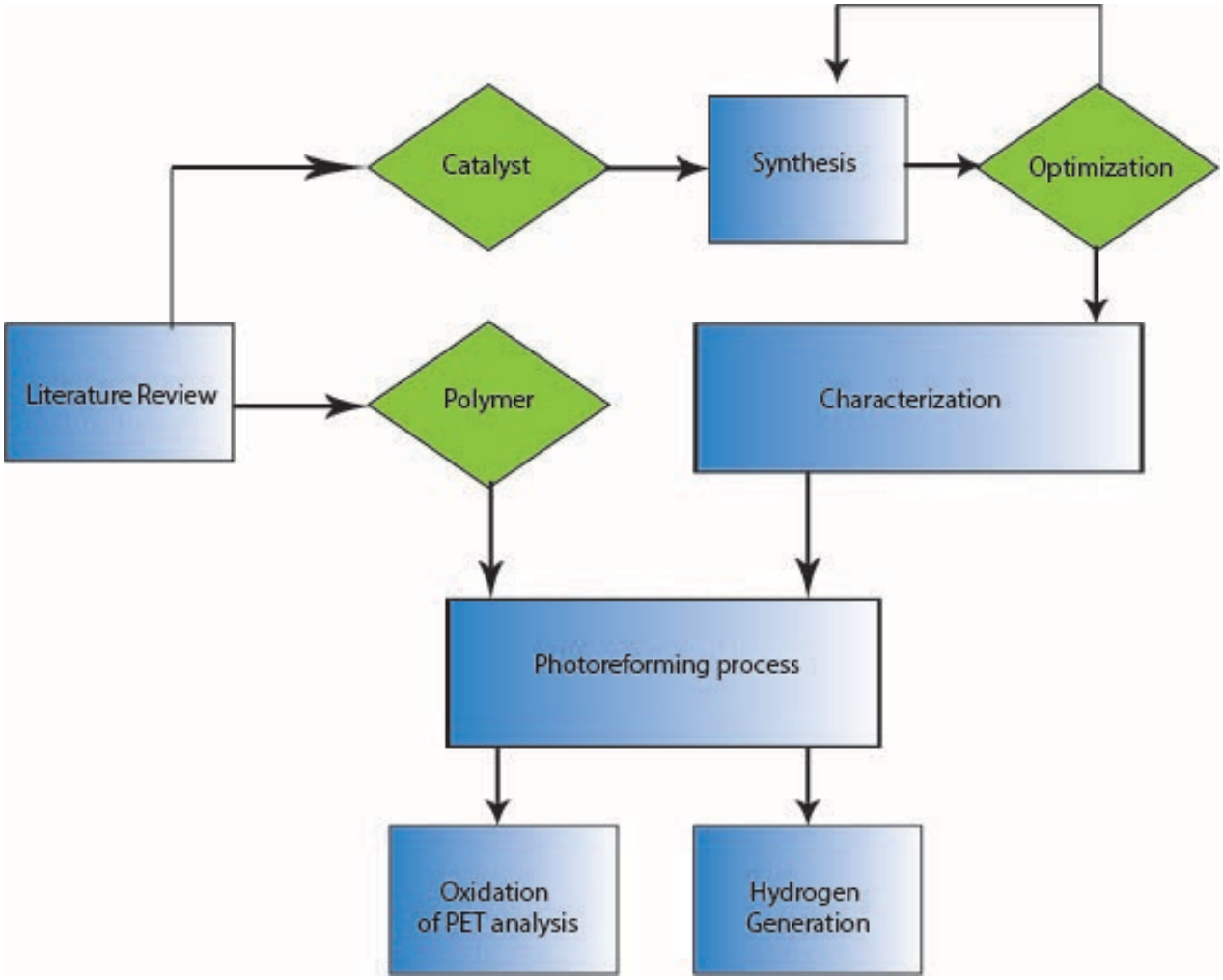

Figure 4: Schematic diagram of experimental plan

Characterization

Structure and morphology of the catalyst doped with Au was characterized by an H-7650 transmission electron microscope (TEM; Hitachi High-Technologies Corp., Pleasanton, CA). Transmission electron microscopy is a useful electron microscopy technique in heterogeneous catalysis for imaging samples on the nanometer scale. Unlike optical microscopy this method does not use photons instead a beam of high energy electrons are utilized. The beam of electrons is accelerated to typically 200 keV and focused using magnetic lenses. These electrons are then transmitted through an ultra-thin specimen and an image is created as the electrons interact with the sample. When studying a supported catalyst TEM analysis operating in bright field mode allows for the measurement of metal NP shape, size, lattice fringes as well as calculation of particle size histograms. Samples for examination by TEM were prepared by placing the dry catalyst powder on

a holey carbon film supported by a 300-mesh copper TEM grid. Crystal phase of the catalyst was studied using X-ray diffraction (XRD; MiniFlex II, Rigaku, Japan). Fourier transform infrared spectroscopy (FTIR) measurements (Nicolet iS10 FT-IR spectrometer, Thermo Fisher Scientific Inc., MA, USA) were performed in the transmittance mode in the spectral range of 600- 4000 cm-1. UV- vis spectrophotometer (DR6000; Hach Company, Loveland, Colorado, USA) was used to collect UV-Visible light absorption spectra.

Photocatalysis experiments

1. Photocatalytic degradation of low-density polyethylene (LDPE) film of size (1 cm × 1 cm) can be carried out on a petri dish containing the photocatalyst and deionized water.
2. Three light sources can be used:
   - A high-pressure UV Mercury Vapor lamp (160W PUV-10, Zoo Med Laboratories, San Luis Obispo, CA)
   - A low-pressure UV lamp (39W T5 HO, Zoo Med Laboratories, San Luis Obispo, CA)
   - A visible light source provided by a fluorescent lamp (40W F40T12/DX, Philips, USA)
3. The irradiance of high-pressure UV lamp concentrates on both UV (minor peaks at 290, 315, 335 nm, and a dominant peak at 365 nm)
4. Visible light (405, 435, and 545 nm) wavelength ranges
5. The irradiance of low-pressure UV lamp is primarily at 253.7 nm

Carbonyl index (CI) and vinyl index (VI) of photocatalyzed microplastics can be calculated to compare the performance of photocatalysts as an indirect quantification of the degree of degradation

Carbonyl index (I_{CO}) can be calculated using,

$$I_{CO} = "(A_{1740} - A_{1835}) \text{ } "/"(0.008 * t)"$$

The IR absorption band at 1740 cm^{-1} (A 1740) and stretching vibration of the carbonyl group (C=O); the absorbance at 1835 cm^{-1} (A_{1835})

where t is the thickness of the sample (mm)

The fluorescent lamp simulates natural sunlight emitting a small amount of UV light (primary peak at 365 nm, and a minor peak at 378 nm), and broad-spectrum range of visible light from 400 to 700 nm with distinct peaks at 405, 436, 488, 546, 577-593, 611, 621, 650, 663 nm

The photon flux density of the light sources can be measured using a quantum sensor (MQ-200, Apogee Instruments, Inc., UT, USA).

Vinyl index (IV) can be calculated using,

ratio of absorbance of the band on 909 cm^{-1} (A_{909}), stretching vibration of the vinyl group $(CH_2{=}CH)_n$, and absorbance at 2020 cm^{-1} "(A_{2020})"

$$I\text{V} = "(A_{909}) \text{ } "/"(A_{2020})"$$

Gas Analysis

- The accumulation of H_2 can be measured via gas chromatography on an Agilent 7890A gas chromatograph equipped with a thermal conductivity detector and HP-5 molecular sieve column using N_2 as the carrier gas.
- Methane (2% CH_4 in N_2) can be used as an internal standard after calibration with different mixtures of known amounts of $H_2/N_2/CH_4$.
- CO_2 detection can be performed with mass spectrometry on a Hiden Analytical HPR-20 benchtop gas analysis system fitted with a custom-designed 8-way microflow capillary inlet to a HAL 101 RC electron impact quadrupolar mass spectrometer with a Faraday detector.

Results

Characterization of catalysts

1. UV-Vis Spectrophotometer

TiO_2/Au, TiO_2/Pt and ZnO/Pt catalysts were developed, and their photocatalytic activity was evaluated considering the UV absorption at wavelength 528 nm. Figure 5 shows the comparison of UV absorption of degraded RB using different catalysts at 528 nm.

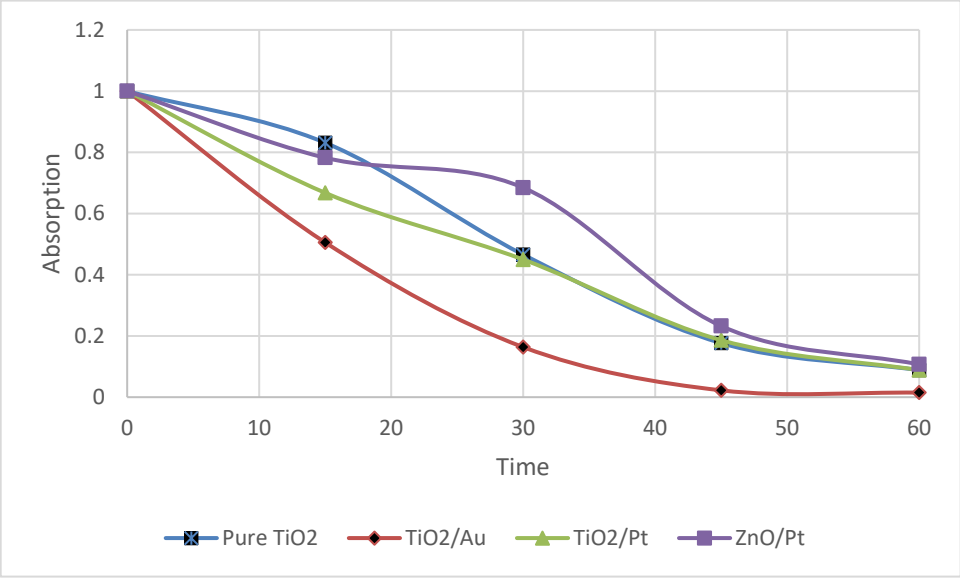

Figure 5: UV absorbance of RB degraded using pure TiO_2, TiO_2/Au, TiO_2/Pt and ZnO/Pt at 528 nm and its variation with time

Figure 5 indicates that photocatalytic activity of modified TiO_2 with Au deposition is higher than the other catalysts. And it performed better than pure TiO_2. Degradation efficiency is highest in TiO_2/Au which is 98% and pure TiO_2 and TiO_2/Pt has similar degradation efficiency of 91%. RB degradation efficiency with ZnO/Pt is 89% which is the lowest compared to other photoactivities.

With these results TiO_2/Au catalyst was considered for further characterization.

Full wavelength scan RB under the TiO_2/Au catalytic action is shown in Figure 6. Color change was observed, and pink colored solution become colorless with time. Each experiment was repeated 5 times and verified the results. Standard deviation of testing trials of pure TiO_2 is 0.1157 and standard deviation of trials for modified TiO_2 (TiO_2/Au) is 0.0495. The absorption decreased gradually to a value near zero. The increase in the absorbance may be explained by the intermediate products of degrading RB absorbing UV–vis light at the wavelength region of RB.

The reaction rate decreases with irradiation time since it follows apparent first-order kinetics and additionally a competition for degradation may occur between the reactant and the intermediate products. Degradation rate of TiO_2/Au is higher than that of the pure TiO_2.

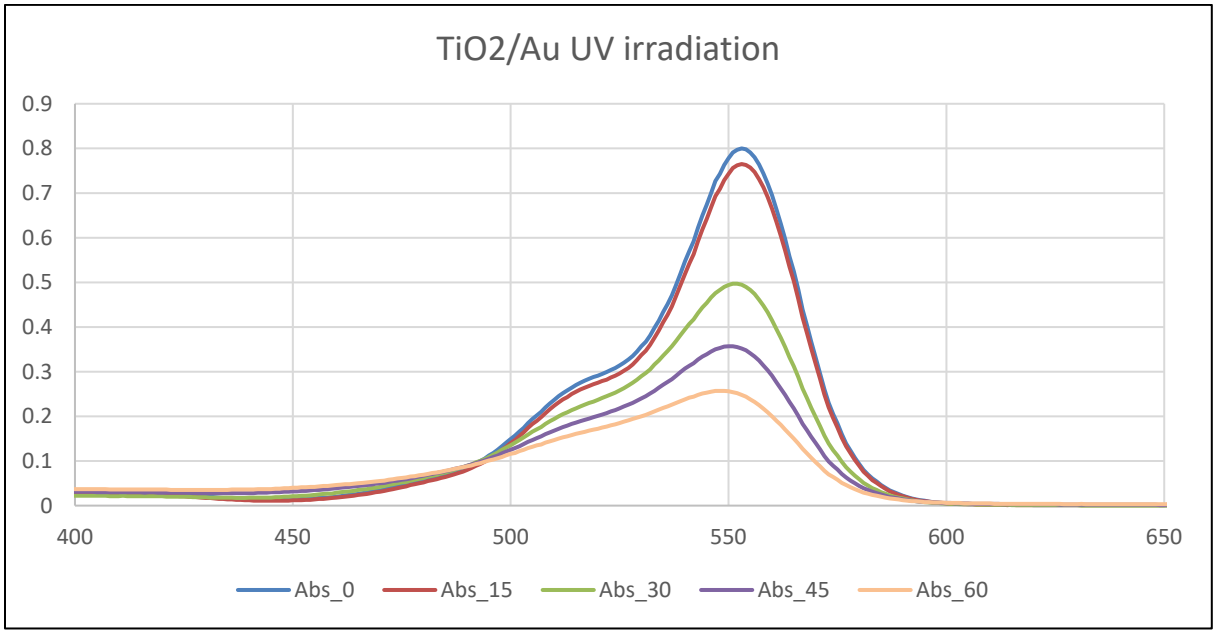

Figure 6: Variation of absorbance spectra of Rhodamine B in the presence of TiO_2/Au nanoparticles with time

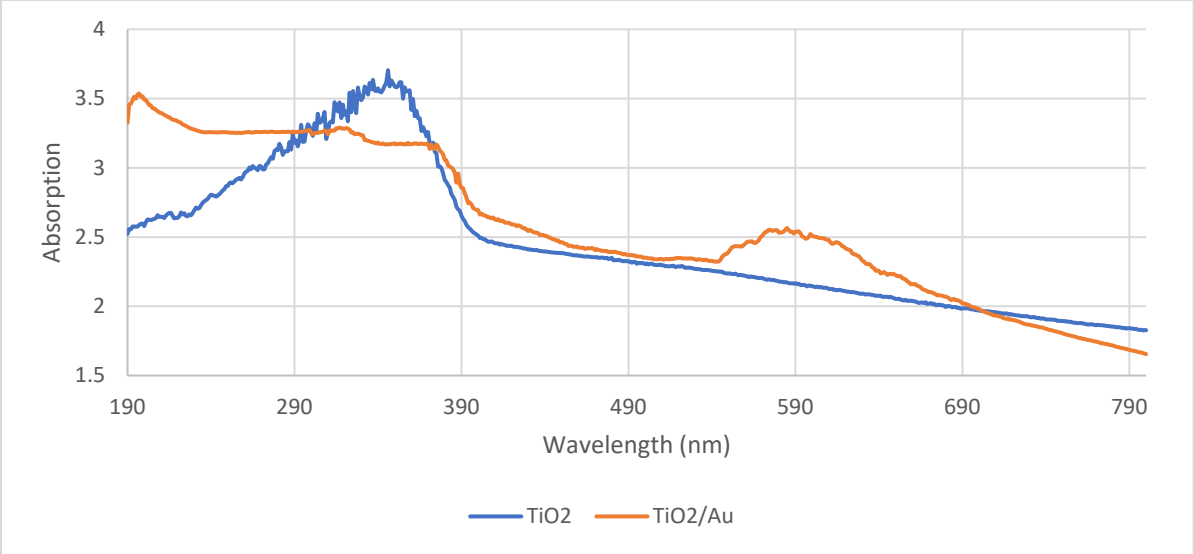

Figure 7: Full wavelength scan using UV spectrophotometer for pure TiO_2 and modified TiO_2/Au

Figure 7 shows the full wavelength spectrum of pure TiO_2 and TiO_2/Au. TiO_2 shows absorption in UV range while indicating a strong peak at wavelength of 350 nm. Compared to the pure TiO_2 absorption spectrum TiO_2/Au shows peak around 580 nm. This is due to the LSPR of Au NPs. Specially, this absorption peak, appearing in visible light region, is responsible for Au/TiO_2 visible light response. Besides, the surface plasmon absorption of Au NPs deposited on TiO_2 surface has a red shift comparing with that of Au NPs immersed into water. The different dielectric constant of environment surrounding the Au NPs causes the red shift [48].

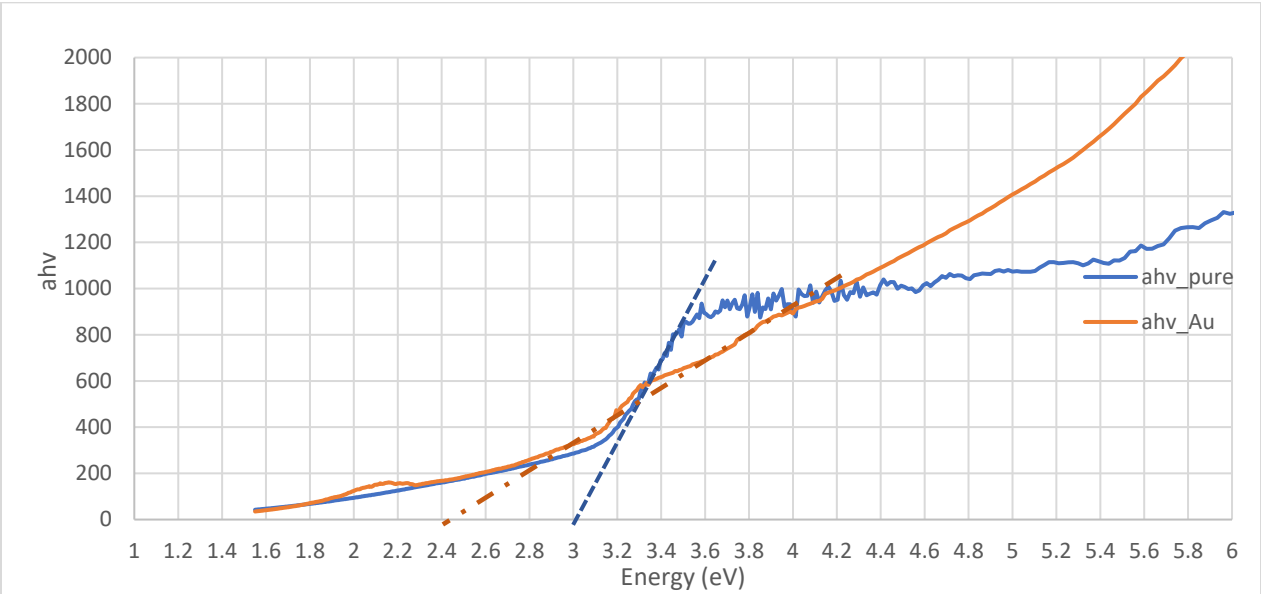

Figure 8: Band gap energy calculation

Band gap calculation was done using Tauc method [49]. Band gap energy of pure TiO_2 is around 3 eV and after gold doping it reduces into 2.4 eV. Pure anatase TiO2 presents a band gap energy of 3.2 eV. In this study, P25 TiO_2 consists of 80% anatase and 20% rutile which justifies the difference. This reduction of band gap energy proves the efficient photocatalytic activity in visible light range while providing required energy for hydrogen producing reduction reaction.

2. X-Ray Diffraction

TiO_2/Au nanoparticles were characterized using powder X-ray diffraction method. X ray diffraction pattern is given in the Figure 9. X ray diffraction data was smoothed using LOESS (locally weighted smoothing) function to remove the noise. LOESS is a popular tool used in regression analysis that creates a smooth line through a time plot or scatter plot to see relationship between variables and foresee trends.

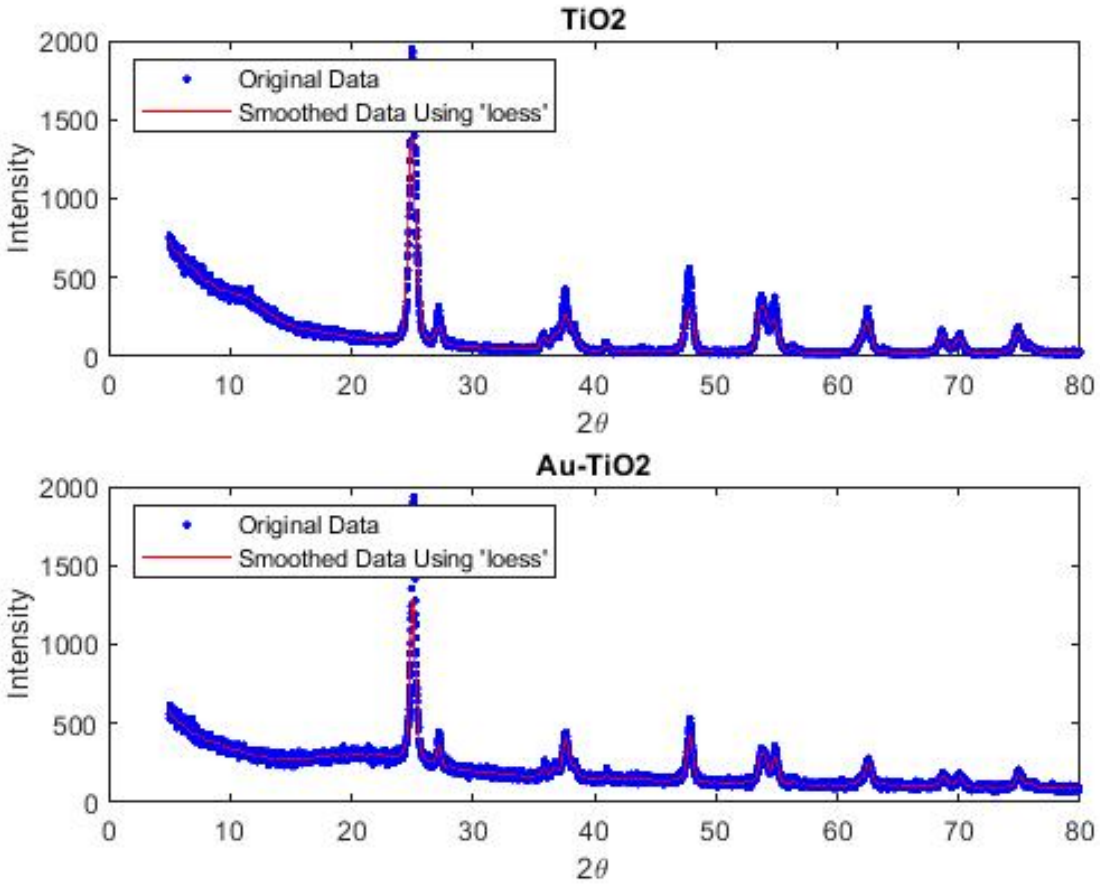

Figure 9: X ray diffraction pattern of pure TiO_2 and TiO_2/Au

There could be seen peaks at positions as shown in the Table 10. It indicates that the pure TiO_2 is consists of rutile and anatase polymorphs of TiO_2.

Table 10: Comparison of peak positions with reported values

Peak positions	Anatase	Rutile	[50]
25.10	25.3		25 A
27.20		27.4	27 R
35.95		36.0	36 R
37.69	37.7		
40.92		41.2	41 R
47.83	48.0		48 A
53.75	53.8		53 R
54.86	55.0		55 A
62.57	62.6		62 A
68.80	68.8		
70.00	70.2		
74.89		74.4	

Characteristic peaks of anatase indexed to (101), (004), (200), (105), (211), and (204) crystal faces. On the other hand, the characteristic diffraction peaks at 2θ angles of 27.0° is assigned to (110) plane of rutile TiO_2. Hence, the synthesized nanocomposites had TiO_2 in the anatase and rutile phases, which was unique to our synthesized materials. Results verified with the literature as shown in the Table 10. Further, peak positions at 37.5°, 65° and 78° 2θ angles were observed. Those peak positions are identical to the crystal phases of gold which indexed to Millar indices of (111), (222) and (311) respectively. It confirms the gold deposition on the TiO_2 crystal structure.

3. TEM images

Further verification of results was done using the TEM analysis. Two samples of pure TiO_2 before modification and TiO_2/Au particles after modification was observed.

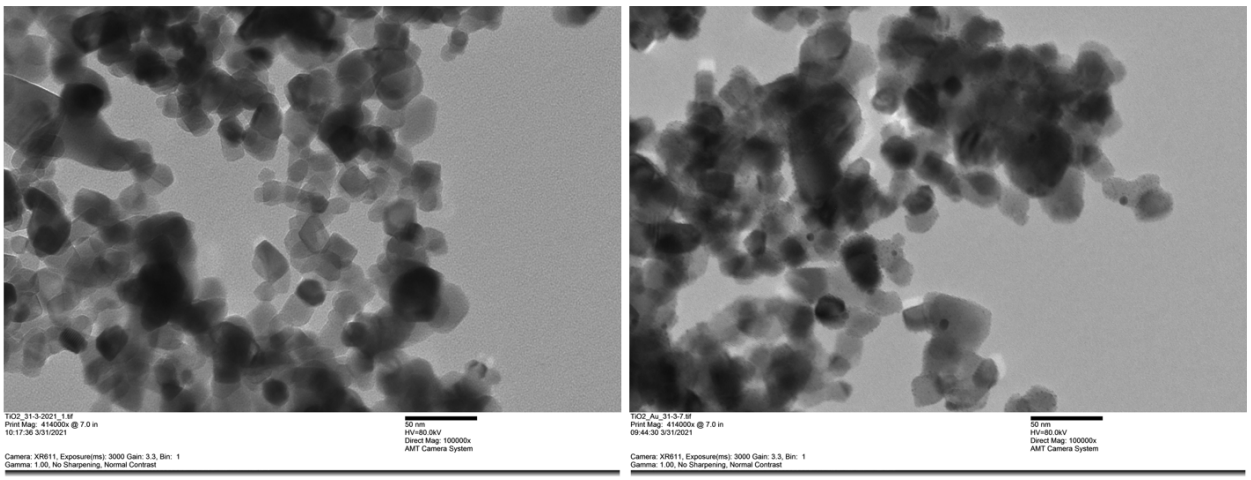

TiO2 TiO2-Au

Figure 10: 100k Magnificat TEM images of modified and unmodified TiO_2

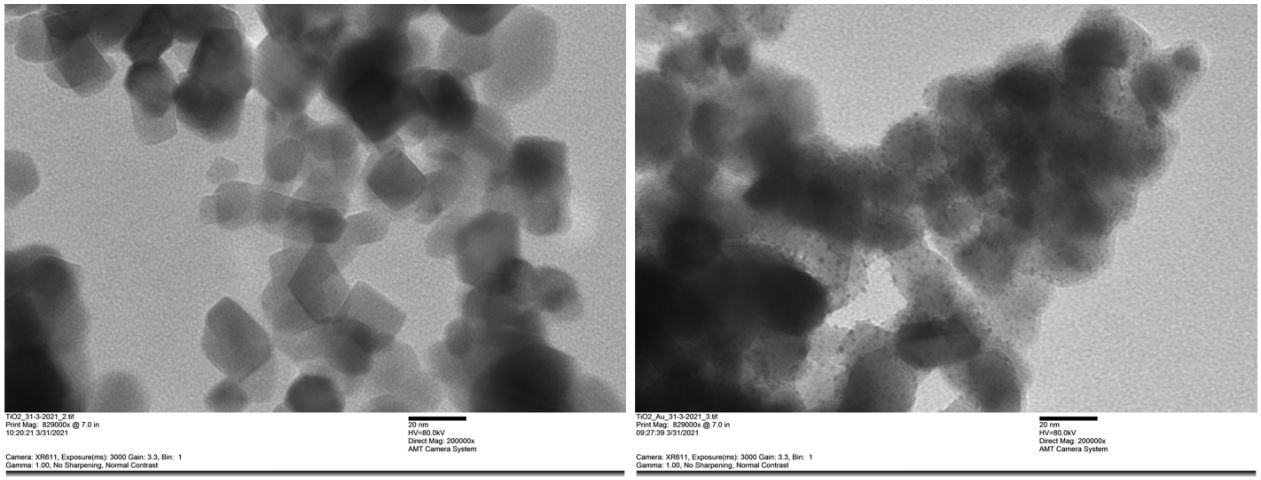

TiO2 TiO2-Au

Figure 11: Comparison of TEM images of modified and unmodified TiO_2 under 200k magnification

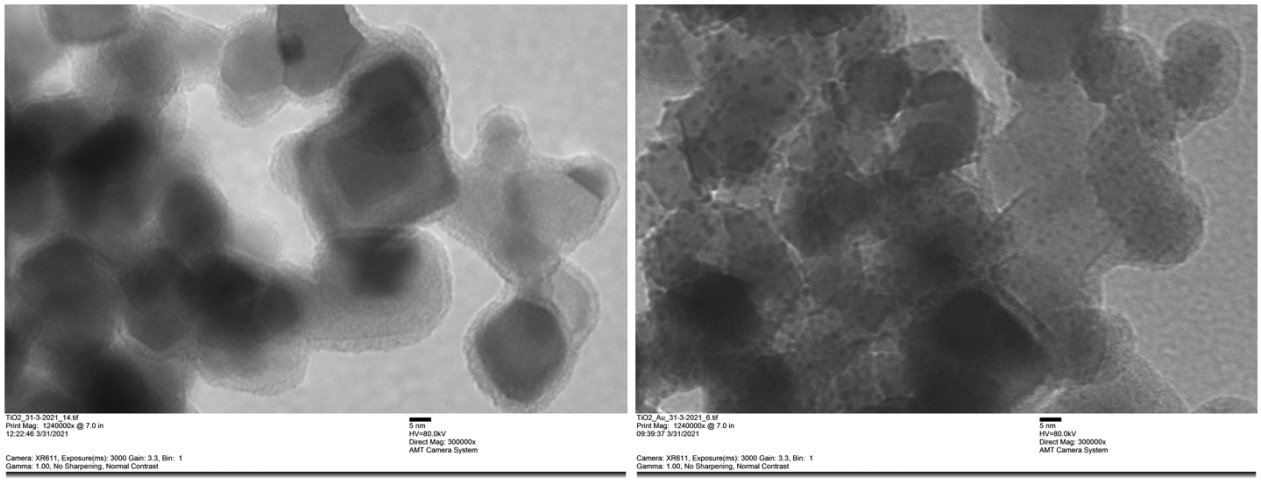

TiO2 TiO2-Au

Figure 12: TEM images of modified and unmodified TiO_2 under 300k magnification

Average size of TiO_2 nanoparticles before gold doping is 20.79 nm and after gold doping it is 21.57 nm. Similarity of these values proves that the TiO_2 particle size does not change due to modification. P25 TiO_2 is known to comprise of small spherical anatase crystallites of average size 20–30 nm, and larger angular rutile crystallites with average size 40–60 nm [51], both of which are evident in the TEM images.

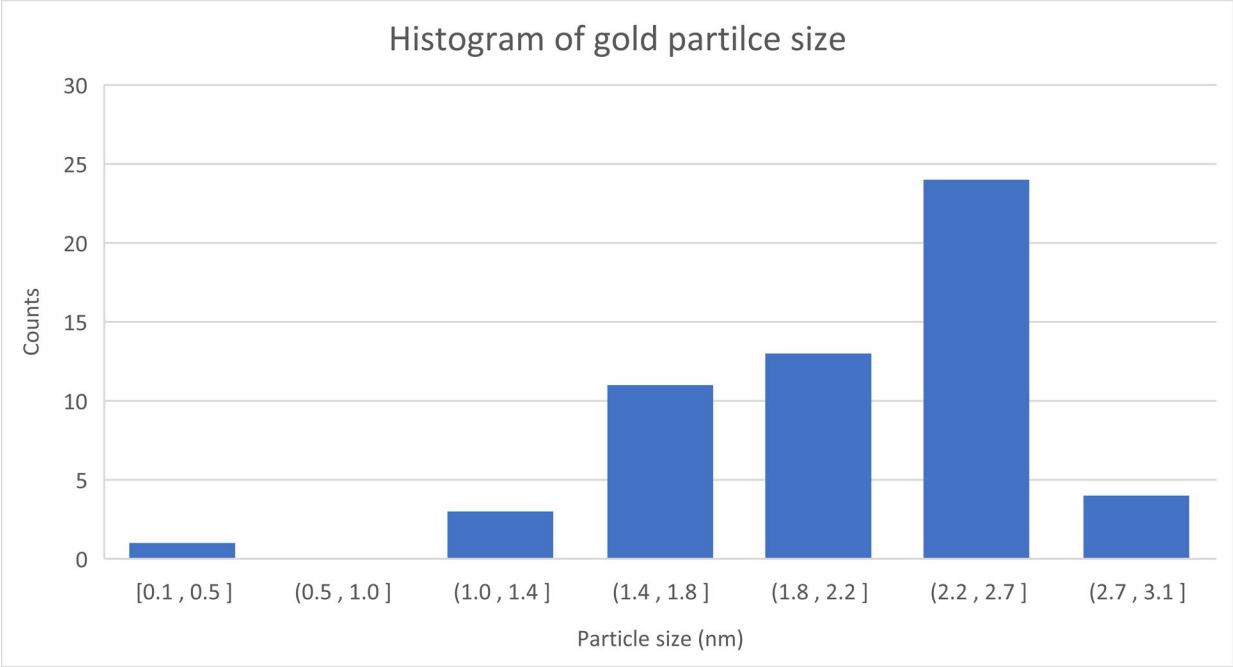

Figure 13: Particle size distribution of doped gold particles on TiO_2 surface

Average gold particle size deposited on TiO_2 is 2 nm. It was also previously reported that smaller size (around 5 nm and smaller) particles exhibit higher photo-, electro-, as well as chemical catalytic activity than larger sized particles. For example, it was shown that Au NPs of size 2–5 nm show specially high activity for oxidation of CO and propylene [52]. So that the average particle size of 2 nm is promising for higher photocatalytic activity.

4. FTIR analysis

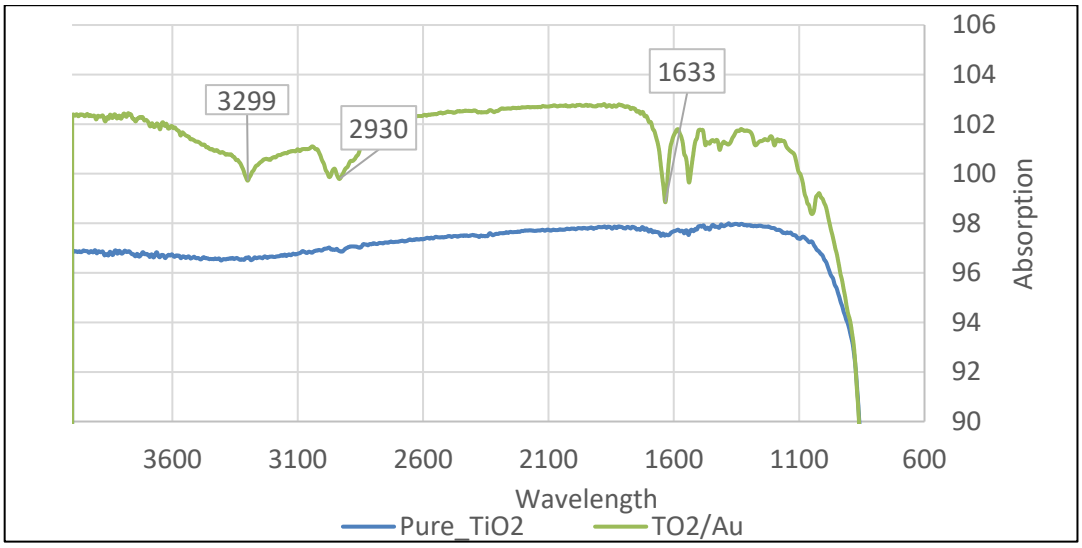

Figure 14: FTIR spectrum of pure TiO_2 and TiO_2 modified with gold deposition

Modification of TiO_2 with gold resulted peak positions at 3425, 2921 and 1631 cm^{-1} [52]. These peaks are due to O-H, CH_3 and N-H functional groups. It indicates that the peak at 3425 cm^{-1} corresponding to the hydrogen bonded hydroxyl groups on the surface of the catalyst is prominently observed in the Au loaded catalysts while it is absent in the bare P25C catalyst. Also, at wavenumbers around 2852 to 2921 cm^{-1} the peak resulting from the water of crystallization is clearly seen in the Au loaded catalysts, while it is not observed in the bare catalyst. A set of peaks around 1630 cm^{-1} are also seen in the Au loaded catalysts and they correspond to the surface adsorbed water.

Photodegradation of microplastics

Figure 15 shows the FTIR spectrum of PET before degradation. Resulting peaks are compared with reported spectrum for PET. With overall agreement of 99.5% it verifies the used PET properties matches with standard PET properties. For the PET, five main peaks are identified at wavenumbers 1715, 1245, 1100, 870 and 730 cm^{-1}, corresponding in ketones (C = O), ether aromatic (C-O), ether aliphatic (C-O), aromatic (C-H) and aromatic (C-H) bond.

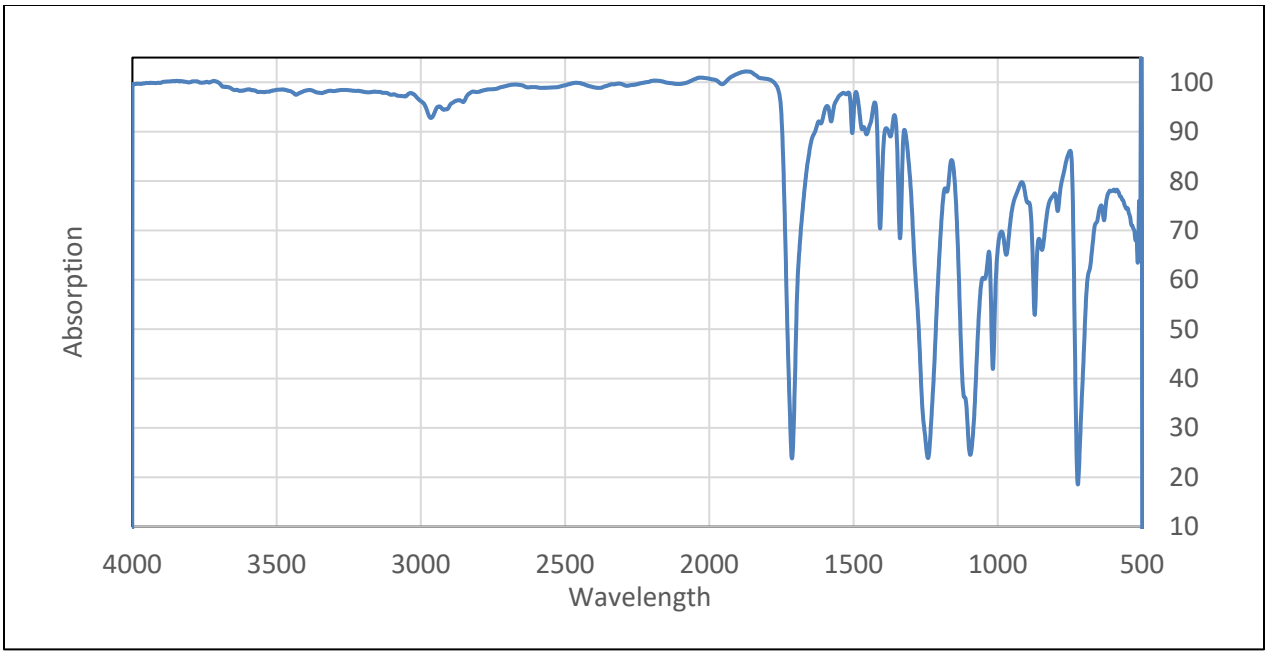

Figure 15: FTIR spectrum of pretreated PET

Table 11: Comparison of used PET with standards

Observed peak position	Standard peak for FTIR of PET	Agreement/(%)
2963	2969	99.7975
2371	2350	99.1143
2104	2100	99.80989
1956	1960	99.7955
1713	1730	99.00759
1573	1577	99.74571
1503	1504	99.93347
1452	1453	99.93113
1338	1342	99.70105
1241	1240	99.91942
1094	1096	99.81718
1015	1050	96.55172
968	972	99.58678
872	872	100
847	848	99.88194
791	795	99.49431
721	712	98.75173
Overall agreement		99.46113

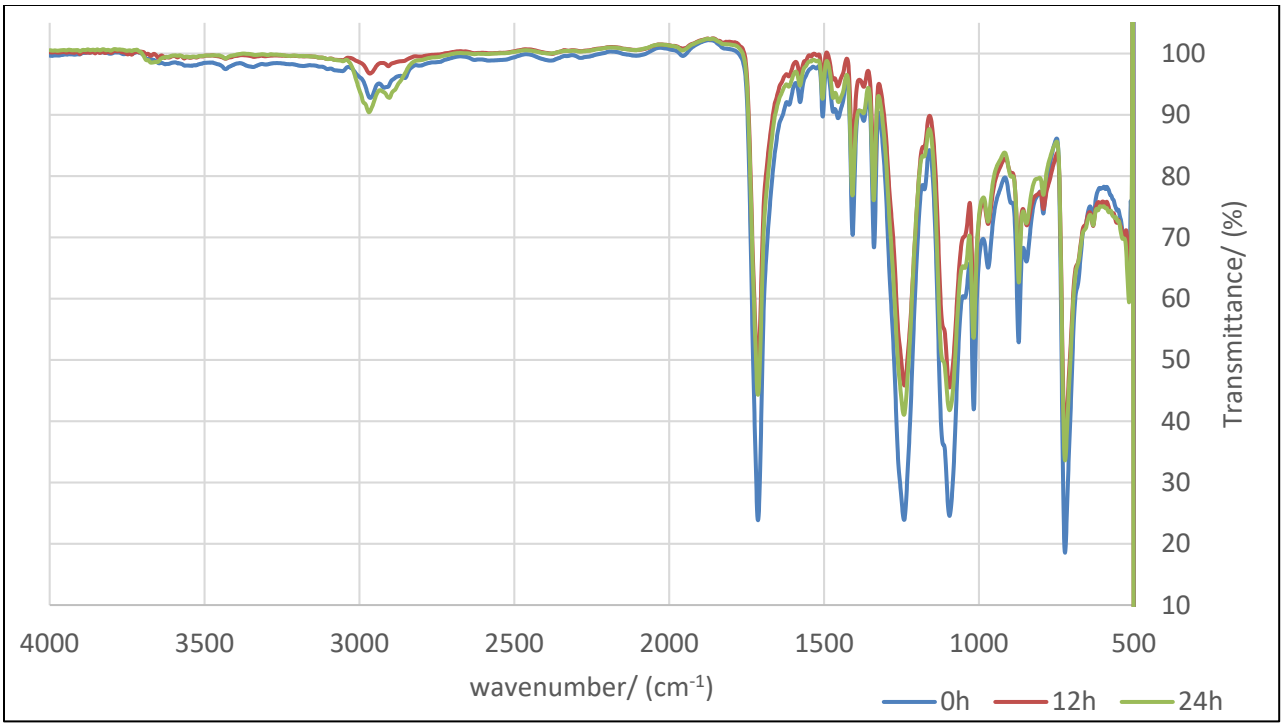

Figure 16: comparison of FTIR spectrum of PET before and after UV irradiation

FTIR spectrum of PET before and after degradation is shown in Figure 16. Peak due to hydroxyl group at 2900 cm^{-1} increased with degradation processes. At 1715 cm^{-1} (C = O), there is a decrease; same for 1245 cm^{-1}; at 1100 cm^{-1}, there is a decrease of peak at 870 cm^{-1}, the aromatic (C-H) is disappearing, while at 730 cm−1, there is a decrease and the peak almost disappears. The outer PET surface also demonstrates new groups, which are not typical for PET.

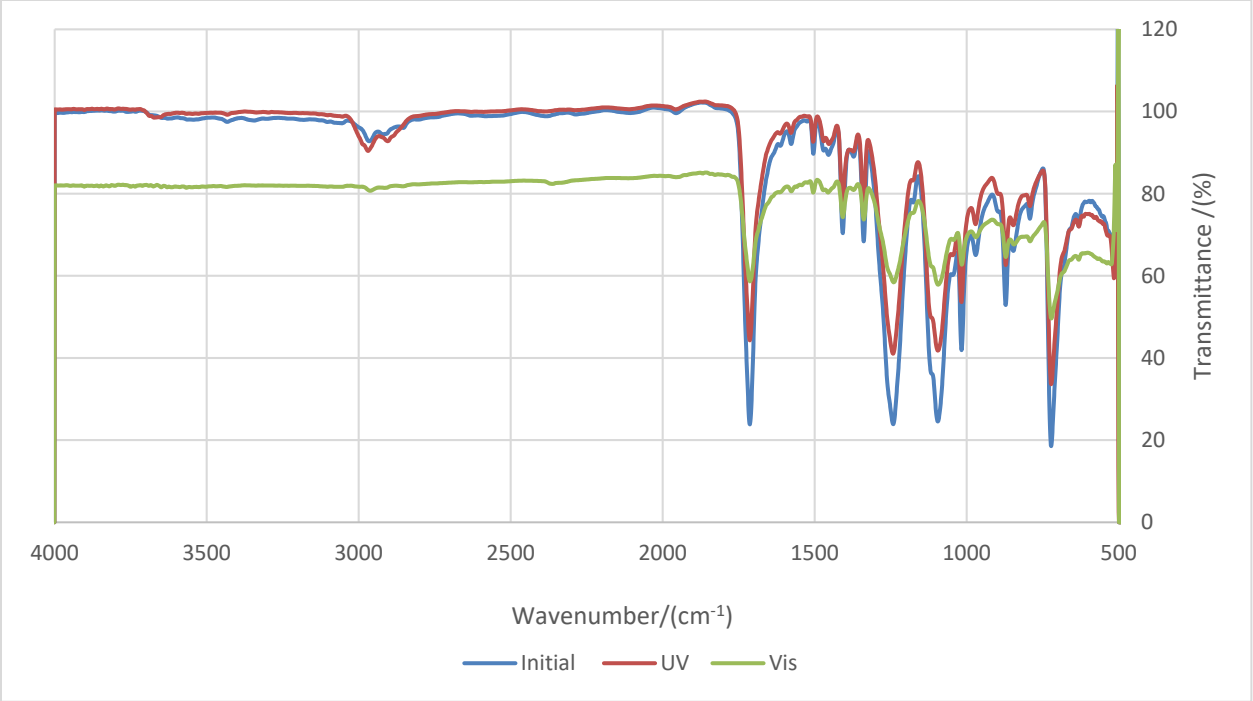

Figure 17: Comparison of PET degradation with TiO_2/Au under UV and Visible light irradiation

PET degradation under UV and visible light irradiation was observed using the same amount of catalyst and same PET weight. Transmittance of most of peak positions decreased with the UV irradiance. Peak in the wavenumber region of hydroxyl group increased under UV irradiance but peak disappears in the visible light irradiated PET spectrum. The further analysis of the FTIR spectrums carbonyl index and vinyl index was calculated. Carbonyl index and the vinyl index reduce after UV and visible light irradiation. It verifies the degradability. But these data are not enough to compare the degradability among the visible and UV irradiation as shown in Tables 12 and 13.

Table 12: Carbonyl index

	Abs 1740	Abs 1835	Thickness/(mm)	Carbonyl index
Initial	-1.87547	-2.00546	0.254	63.96971
UV	-1.91368	-2.00775	0.254	46.29355
Vis	-1.87964	-1.92836	0.254	23.97716

Table 13: Vinyl index

	Abs 909	Abs 2020	Vinyl index
Initial	-1.89684	-2.00387	0.946589
UV	-1.91794	-2.00627	0.955975

Vis	-1.86601	-1.92584	0.968934

Microscopic images

Optical microscope was used to observe the surface changes of plastics before and after UV irradiation. Figure 18 Shows the surface morphology of 10 times magnified image of PET at the initial stage, after 12h UV exposure and after 24h UV irradiation under 10 times magnification. 20 times and 40 times magnified images of PET before and after UV irradiation is given in Figure 18, 19 and figure 20 respectively. Surface morphology changes with cracks are observed in PET particles.

It can be concluded that there is a degradation of plastics after UV irradiation under catalytic action.

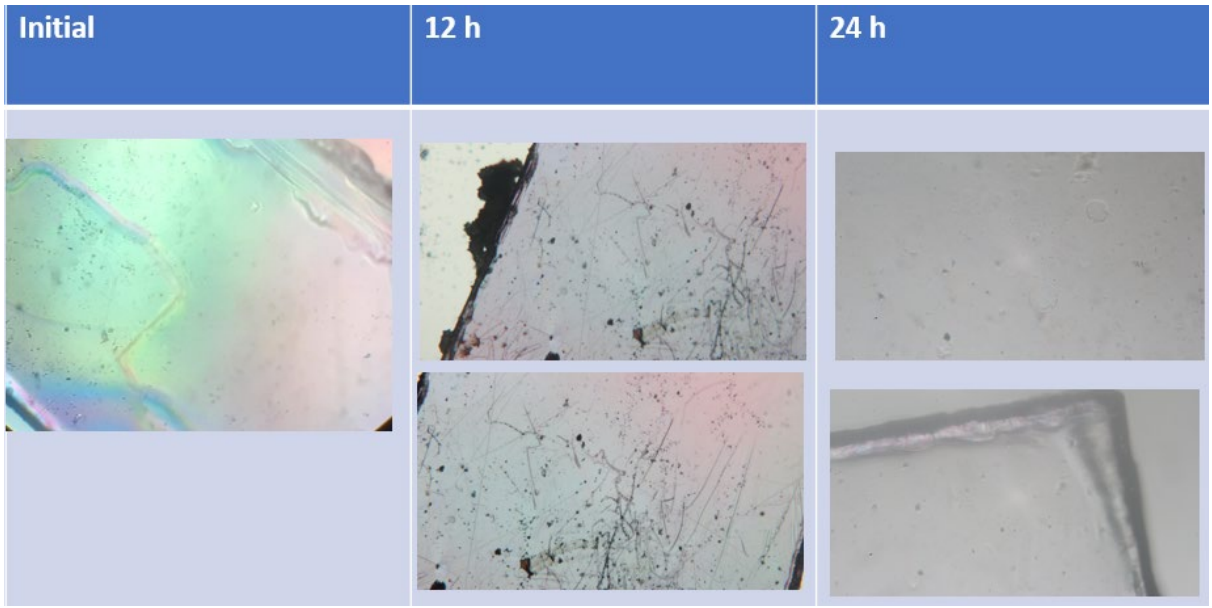

Figure 18: 10 times magnified images showing surface morphology changes of PET before and after UV irradiance

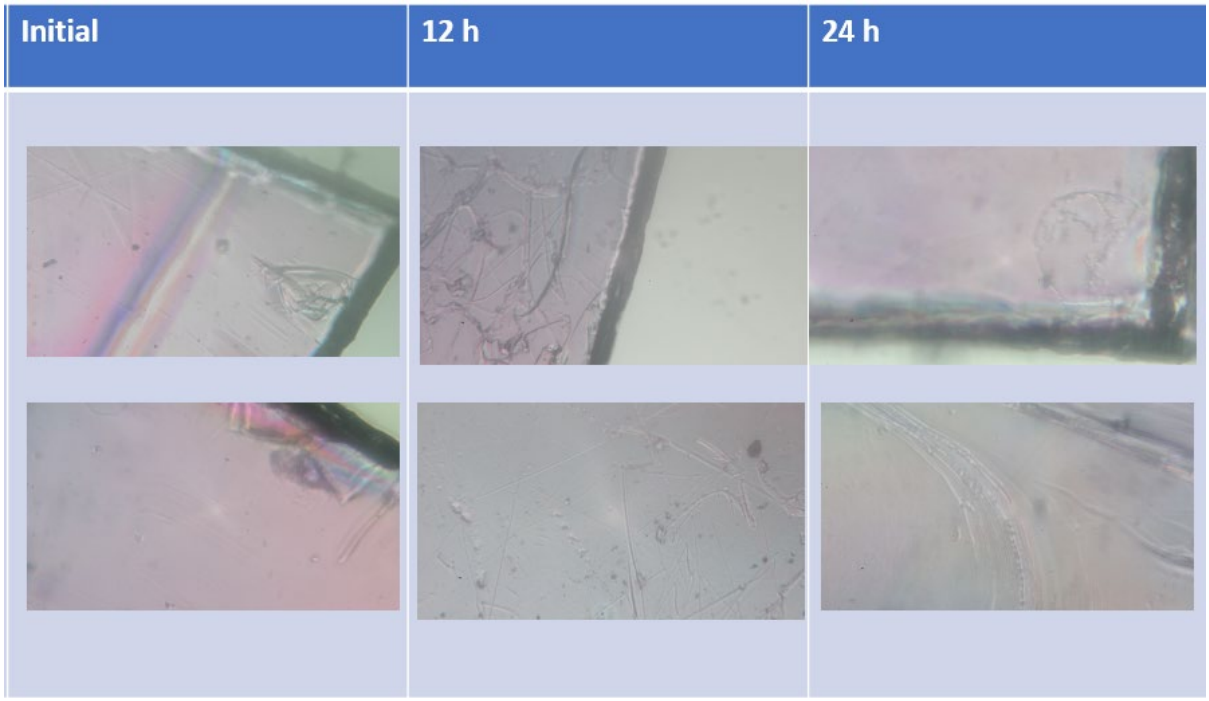

Figure 19: 20 times magnified images of PET particles before degradation and after 12 h and 24 h UV irradiation

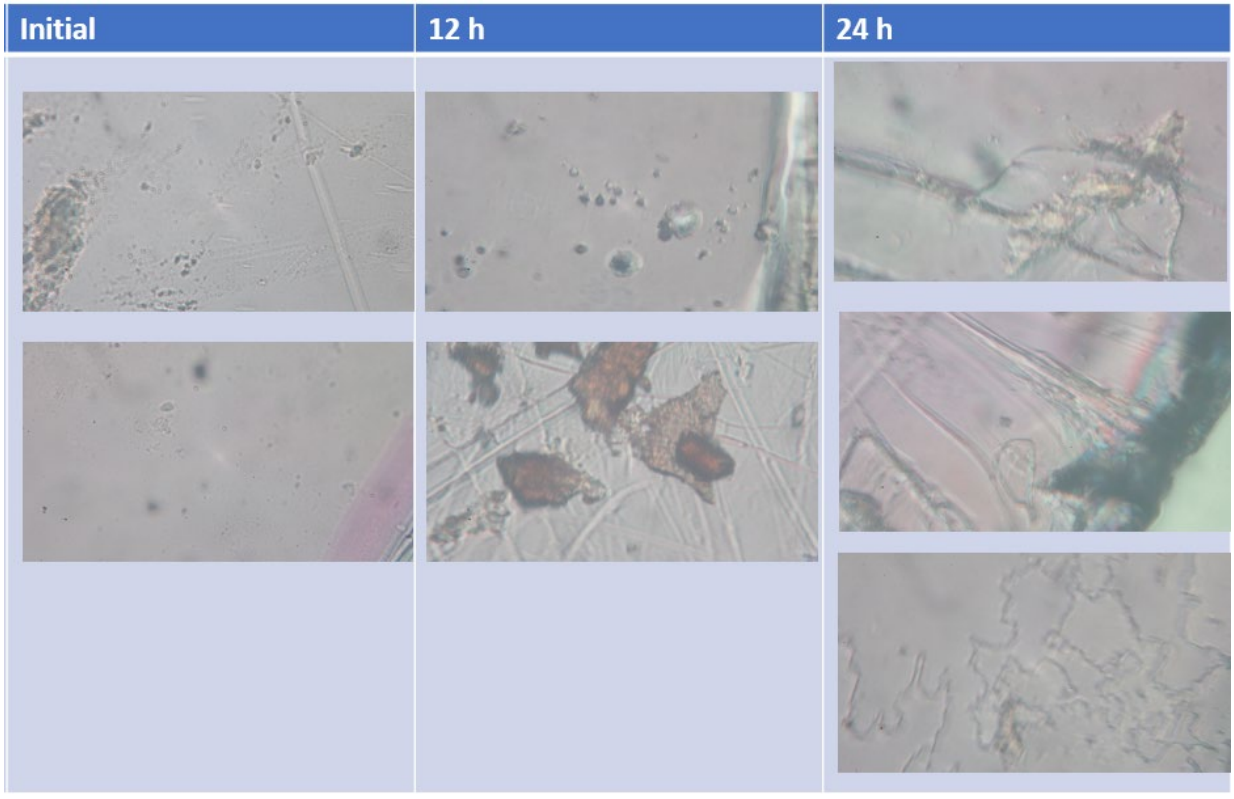

Figure 20: 40 times magnified images of PET particles before degradation and after 12 h and 24 h UV irradiation

Hydrogen production

Hydrogen production was first evident by the air bubbles present in the surface of the plastic particles and the reactor walls.

Figure 21: Petri dish with reactor solution before UV irradiating

Figure 22: Presence of air bubbles in the reaction solution during UV irradiation

Figure 23: Bubbles present in the bottom surface of the floating PET particles

Gas production is evident with the bubble generation with the reaction. Gas identification and quatification is the next step of the process. A reactor has been designed to collect and GC-MS with a TCD is proposed to use in characterizing and measuring the gases. Collected gas within 1 hour intervals of the reaction time will be manually injected to the GC-MS. Agilent 7890A gas chromatograph equipped with a thermal conductivity detector and HP-5 molecular sieve column using N_2 as the carrier gas will be used for the analysis.

6. Provide a paragraph on who will benefit from your research results. Include any water agency that could use your results.

Microplastic pollution of water has been a global challenge. This study aims to develop highly functional nanocomposite photocatalysts to clean water and convert microplastics from a waste to H2 energy. This research will help improve water quality and reduce acute and chronic toxicity to human and aquatic life. The study will assist in guiding the potential application of photocatalysis for environmental remediation of microplastic pollution.

7. Describe how you have spent your grant funds. Also provide your budget balance and how you will use any remaining funds. If you anticipate any funds remaining after May 15, 2020, please contact Carolina Mijares immediately. (575-646-7991; mijares@nmsu.edu)
   The research fund was spent as planned and used before May 15, 2020

8. List presentations you have made related to the project.
   Poster presentation in NM WRRI conference in Oct 2020.
   Flash presentation in 17th annual RMSAWWA/RMWEA student conference in May 2021.

9. List publications or reports, if any, that you are preparing. Remember to acknowledge the NM WRRI funding in any presentation or report that you prepare.
   None.

10. List any other students or faculty members who have assisted you with your project.
    Dr. Stefan Zollner
    Dr. William Maio

11. Provide special recognition awards or notable achievements as a result of the research including any publicity such as newspaper articles, or similar.
    People's choice Brown & Caldwell flash presentation award at the 17th annual RMSAWWA/RMWEA student conference

12. Provide information on degree completion and future career plans. Funding for student grants comes from the New Mexico Legislature and legislators are interested in whether recipients of these grants go on to complete academic degrees and work in a water-related field in New Mexico or elsewhere.
    Edirisooriya, E.M.N.T. is a Master student in her first academic year. She will continue an academic carrier related to water after graduation in future.

References

[1] M. Kosuth, S. A. Mason, and E. V. Wattenberg, "Anthropogenic contamination of tap water, beer, and sea salt," *PLoS One*, vol. 13, no. 4, 2018, doi: 10.1371/journal.pone.0194970.

[2] J. Jambeck *et al.*, "the Ocean : the Ocean :," vol. 347, no. 6223, pp. 3–6, 2015, doi: 10.1126/science.1260352.

[3] T. S. Tofa, K. L. Kunjali, S. Paul, and J. Dutta, "Visible light photocatalytic degradation of microplastic residues with zinc oxide nanorods," *Environ. Chem. Lett.*, vol. 17, no. 3, pp. 1341–1346, 2019, doi: 10.1007/s10311-019-00859-z.

[4] T. Uekert, H. Kasap, and E. Reisner, "Photoreforming of Nonrecyclable Plastic Waste over a Carbon Nitride/Nickel Phosphide Catalyst," *J. Am. Chem. Soc.*, vol. 141, no. 38, pp. 15201–15210, 2019, doi: 10.1021/jacs.9b06872.

[5] A. D. Levine, G. Tchobanoglous, and T. Asano, "Size distributions of particulate contaminants in wastewater and their impact on treatability," *Water Res.*, vol. 25, no. 8, pp. 911–922, 1991, doi: 10.1016/0043-1354(91)90138-G.

[6] E. Dulekgurgen, S. Doğruel, Ö. Karahan, and D. Orhon, "Size distribution of wastewater COD fractions as an index for biodegradability," *Water Res.*, vol. 40, no. 2, pp. 273–282, 2006, doi: 10.1016/j.watres.2005.10.032.

[7] F. Collard *et al.*, "Anthropogenic particles in the stomach contents and liver of the freshwater fish Squalius cephalus," *Sci. Total Environ.*, vol. 643, pp. 1257–1264, 2018, doi: 10.1016/j.scitotenv.2018.06.313.

[8] T. Uekert, M. F. Kuehnel, D. W. Wakerley, and E. Reisner, "Plastic waste as a feedstock

for solar-driven H2 generation," *Energy Environ. Sci.*, vol. 11, no. 10, pp. 2853–2857, 2018, doi: 10.1039/c8ee01408f.
[9] A. Cózar *et al.*, "Plastic debris in the open ocean," *Proc. Natl. Acad. Sci. U. S. A.*, vol. 111, no. 28, pp. 10239–10244, 2014, doi: 10.1073/pnas.1314705111.
[10] A. Dyachenko, J. Mitchell, and N. Arsem, "Extraction and identification of microplastic particles from secondary wastewater treatment plant (WWTP) effluent," *Anal. Methods*, vol. 9, no. 9, pp. 1412–1418, 2017, doi: 10.1039/c6ay02397e.
[11] R. M. Goldwyn, "Comment," *Gen. Hosp. Psychiatry*, vol. 5, no. 1, pp. 29–30, 1983, doi: 10.1016/0163-8343(83)90040-3.
[12] S. A. Mason *et al.*, "Microplastic pollution is widely detected in US municipal wastewater treatment plant effluent," *Environ. Pollut.*, vol. 218, pp. 1045–1054, 2016, doi: 10.1016/j.envpol.2016.08.056.
[13] M. Pivokonsky, L. Cermakova, K. Novotna, P. Peer, T. Cajthaml, and V. Janda, "Occurrence of microplastics in raw and treated drinking water," *Sci. Total Environ.*, vol. 643, pp. 1644–1651, 2018, doi: 10.1016/j.scitotenv.2018.08.102.
[14] M. Revel, A. Châtel, and C. Mouneyrac, "Micro(nano)plastics: A threat to human health?," *Curr. Opin. Environ. Sci. Heal.*, vol. 1, no. February, pp. 17–23, 2018, doi: 10.1016/j.coesh.2017.10.003.
[15] A. Beljanski, C. Cole, F. Fuxa, E. Setiawan, and H. Singh, "Efficiency and effectiveness of a low-cost, self-cleaning microplastic filtering system for wastewater treatment plants.," *30th Natl. Conf. Undergrad. Res.*, no. 2016, pp. 1388–1395, 2016, [Online]. Available: http://www.ncurproceedings.org/ojs/index.php/NCUR2016/article/download/2064/1021.
[16] A. Wegner, E. Besseling, E. M. Foekema, P. Kamermans, and A. A. Koelmans, "Effects of nanopolystyrene on the feeding behavior of the blue mussel (Mytilus edulis L.)," *Environ. Toxicol. Chem.*, vol. 31, no. 11, pp. 2490–2497, 2012, doi: 10.1002/etc.1984.
[17] F. Zhang, Z. Wang, S. Wang, H. Fang, and D. Wang, "Aquatic behavior and toxicity of polystyrene nanoplastic particles with different functional groups: Complex roles of pH, dissolved organic carbon and divalent cations," *Chemosphere*, vol. 228, pp. 195–203, 2019, doi: 10.1016/j.chemosphere.2019.04.115.
[18] J. Gigault *et al.*, "Current opinion: What is a nanoplastic?," *Environ. Pollut.*, vol. 235, pp. 1030–1034, 2018, doi: 10.1016/j.envpol.2018.01.024.
[19] W. Panunto *et al.*, "Acute and chronic toxicity studies of the water extract from dried fruits of Terminalia chebula Rezt. in rats," *Int. J. Appl. Res. Nat. Prod.*, vol. 3, no. 4, pp. 36–43, 2010.
[20] L. Wollenberger, B. Halling-Sørensen, and K. O. Kusk, "Acute and chronic toxicity of veterinary antibiotics to Daphnia magna," *Chemosphere*, vol. 40, no. 7, pp. 723–730, 2000, doi: 10.1016/S0045-6535(99)00443-9.
[21] Xiaomi Tong and K. D. Caldwell, "Separation and characterization of red blood cells with different membrane deformability using steric field-flow fractionation," *J. Chromatogr. B Biomed. Sci. Appl.*, vol. 674, no. 1, pp. 39–47, 1995, doi: 10.1016/0378-4347(95)00297-0.
[22] H. P. Van Leeuwen, J. Buffle, and M. Lovric, "Reactant adsorption in analytical pulse voltammetry: Methodology and recommendations (Technical Report)," *Pure Appl. Chem.*, vol. 64, no. 7, pp. 1015–1028, 1992, doi: 10.1351/pac199264071015.
[23] M. V Novotny, "Capillary biomolecular separations," *J. Chromatogr. B Biomed. Sci. Appl.*, vol. 689, no. 1, pp. 55–70, 1997, doi: https://doi.org/10.1016/S0378-4347(96)00398-2.

[24] V. Godoy, M. A. Martín-Lara, M. Calero, and G. Blázquez, “Physical-chemical characterization of microplastics present in some exfoliating products from Spain,” *Mar. Pollut. Bull.*, vol. 139, no. December 2018, pp. 91–99, 2019, doi: 10.1016/j.marpolbul.2018.12.026.
[25] A. Käppler *et al.*, “Analysis of environmental microplastics by vibrational microspectroscopy: FTIR, Raman or both?,” *Anal. Bioanal. Chem.*, vol. 408, no. 29, pp. 8377–8391, 2016, doi: 10.1007/s00216-016-9956-3.
[26] K. Munno, H. De Frond, B. O. Donnell, and C. M. Rochman, “Increasing the Accessibility for Characterizing Microplastics: Introducing New Application-Based and Spectral Libraries of Plastic Particles (SLoPP and SLoPP-E),” no. January, 2020, doi: 10.1021/acs.analchem.9b03626.
[27] I. F. Kadikova, E. A. Morozova, T. V Yuryeva, I. A. Grigorieva, and V. A. Yuryev, “Glass depolymerization in the process of long-term corrosion: A study of deteriorating semiopaque turquoise glass beads using micro-FTIR spectroscopy,” *Mater. Res. Express*, 2020, doi: 10.1088/2053-1591/ab7510.
[28] M. Ballauff and Y. Lu, “‘Smart’ nanoparticles: Preparation, characterization and applications,” *Polymer (Guildf).*, vol. 48, no. 7, pp. 1815–1823, 2007, doi: 10.1016/j.polymer.2007.02.004.
[29] T. Rocha-Santos and A. C. Duarte, “A critical overview of the analytical approaches to the occurrence, the fate and the behavior of microplastics in the environment,” *TrAC - Trends Anal. Chem.*, vol. 65, pp. 47–53, 2015, doi: 10.1016/j.trac.2014.10.011.
[30] Q. Zhou, S. E. Cabaniss, and P. A. Maurice, “Considerations in the use of high-pressure size exclusion chromatography (HPSEC) for determining molecular weights of aquatic humic substances,” *Water Res.*, vol. 34, no. 14, pp. 3505–3514, 2000, doi: 10.1016/S0043-1354(00)00115-9.
[31] A. M. Hansen, T. E. C. Kraus, B. A. Pellerin, J. A. Fleck, B. D. Downing, and B. A. Bergamaschi, “Optical properties of dissolved organic matter (DOM): Effects of biological and photolytic degradation,” pp. 1015–1032, 2016, doi: 10.1002/lno.10270.
[32] S. A. Carr, J. Liu, and A. G. Tesoro, “Transport and fate of microplastic particles in wastewater treatment plants,” *Water Res.*, vol. 91, pp. 174–182, 2016, doi: 10.1016/j.watres.2016.01.002.
[33] B. Ma, W. Xue, C. Hu, H. Liu, J. Qu, and L. Li, “Characteristics of microplastic removal via coagulation and ultrafiltration during drinking water treatment,” *Chem. Eng. J.*, vol. 359, no. September 2018, pp. 159–167, 2019, doi: 10.1016/j.cej.2018.11.155.
[34] J. Talvitie, A. Mikola, A. Koistinen, and O. Setälä, “Solutions to microplastic pollution – Removal of microplastics from wastewater effluent with advanced wastewater treatment technologies,” *Water Res.*, vol. 123, no. July, pp. 401–407, 2017, doi: 10.1016/j.watres.2017.07.005.
[35] M. Claessens, L. Van Cauwenberghe, M. B. Vandegehuchte, and C. R. Janssen, “New techniques for the detection of microplastics in sediments and field collected organisms,” *Mar. Pollut. Bull.*, vol. 70, no. 1–2, pp. 227–233, 2013, doi: 10.1016/j.marpolbul.2013.03.009.
[36] J. Grbic, B. Nguyen, E. Guo, J. B. You, D. Sinton, and C. M. Rochman, “Magnetic Extraction of Microplastics from Environmental Samples,” *Environ. Sci. Technol. Lett.*, vol. 6, no. 2, pp. 68–72, 2019, doi: 10.1021/acs.estlett.8b00671.

[37] A. Misra *et al.*, “Water Purification and Microplastics Removal Using Magnetic Polyoxometalate-Supported Ionic Liquid Phases (magPOM-SILPs),” *Angew. Chemie - Int. Ed.*, vol. 59, no. 4, pp. 1601–1605, 2020, doi: 10.1002/anie.201912111.
[38] F. Liu, N. B. Nord, K. Bester, and J. Vollertsen, “Microplastics removal from treated wastewater by a biofilter,” *Waters*, pp. 1–11, 2020.
[39] C. Cunha, L. Silva, J. Paulo, M. Faria, N. Nogueira, and N. Cordeiro, “Microalgal-based biopolymer for nano- and microplastic removal: a possible biosolution for wastewater treatment,” *Environ. Pollut.*, vol. 263, 2020, doi: 10.1016/j.envpol.2020.114385.
[40] Z. Wang, T. Lin, and W. Chen, “Occurrence and removal of microplastics in an advanced drinking water treatment plant (ADWTP),” *Sci. Total Environ.*, vol. 700, p. 134520, 2020, doi: 10.1016/j.scitotenv.2019.134520.
[41] C. B. Ong, L. Y. Ng, and A. W. Mohammad, “A review of ZnO nanoparticles as solar photocatalysts: Synthesis, mechanisms and applications,” *Renew. Sustain. Energy Rev.*, vol. 81, no. July 2016, pp. 536–551, 2018, doi: 10.1016/j.rser.2017.08.020.
[42] J. Talvitie, A. Mikola, A. Koistinen, and O. Setälä, “Solutions to microplastic pollution – Removal of microplastics from wastewater effluent with advanced wastewater treatment technologies,” *Water Res.*, 2017, doi: 10.1016/j.watres.2017.07.005.
[43] G. Imoberdorf and M. Mohseni, “Modeling and experimental evaluation of vacuum-UV photoreactors for water treatment,” *Chem. Eng. Sci.*, vol. 66, no. 6, pp. 1159–1167, 2011, doi: 10.1016/j.ces.2010.12.020.
[44] M. Bagheri and M. Mohseni, “Computational fluid dynamics (CFD) modeling of VUV/UV photoreactors for water treatment,” *Chem. Eng. J.*, vol. 256, pp. 51–60, 2014, doi: 10.1016/j.cej.2014.06.068.
[45] M. Cargnello *et al.*, “Engineering titania nanostructure to tune and improve its photocatalytic activity,” *Proc. Natl. Acad. Sci. U. S. A.*, vol. 113, no. 15, pp. 3966–3971, 2016, doi: 10.1073/pnas.1524806113.
[46] F. Moreau and G. C. Bond, “Gold on titania catalysts, influence of some physicochemical parameters on the activity and stability for the oxidation of carbon monoxide,” *Appl. Catal. A Gen.*, vol. 302, no. 1, pp. 110–117, 2006, doi: 10.1016/j.apcata.2005.12.031.
[47] S. R. Lingampalli, U. K. Gautam, and C. N. R. Rao, “<C3Ee42623H.Pdf>,” pp. 1–7, 2013.
[48] Z. Lin *et al.*, “On the role of localized surface plasmon resonance in UV-Vis light irradiated Au/TiO2 photocatalysis systems: Pros and cons,” *Nanoscale*, vol. 7, no. 9, pp. 4114–4123, 2015, doi: 10.1039/c4nr06929c.
[49] P. Makuła, M. Pacia, and W. Macyk, “How To Correctly Determine the Band Gap Energy of Modified Semiconductor Photocatalysts Based on UV-Vis Spectra,” *J. Phys. Chem. Lett.*, vol. 9, no. 23, pp. 6814–6817, 2018, doi: 10.1021/acs.jpclett.8b02892.
[50] L. Lin, H. Wang, H. Luo, and P. Xu, “Enhanced photocatalysis using side-glowing optical fibers coated with Fe-doped TiO2 nanocomposite thin films,” *J. Photochem. Photobiol. A Chem.*, vol. 307–308, no. September 2018, pp. 88–98, 2015, doi: 10.1016/j.jphotochem.2015.04.010.
[51] V. Jovic, W. T. Chen, D. Sun-Waterhouse, M. G. Blackford, H. Idriss, and G. I. N. Waterhouse, “Effect of gold loading and TiO2 support composition on the activity of Au/TiO2 photocatalysts for H2 production from ethanol–water mixtures,” *J. Catal.*, vol. 305, pp. 307–317, 2013, doi: 10.1016/j.jcat.2013.05.031.
[52] A. Das, P. Dagar, S. Kumar, and A. K. Ganguli, “Effect of Au nanoparticle loading on the

photo-electrochemical response of Au–P25–TiO2 catalysts," *J. Solid State Chem.*, vol. 281, no. July 2019, p. 121051, 2020, doi: 10.1016/j.jssc.2019.121051.